

First we would like to thank the reviewer, Dr. Hiren Jethva, who took a major part in the improvement of this article. Particularly, we modify the whole section 2.4 to discuss the potential errors induced by the assumption made in the retrieval and especially the one concerning the weak sensitivity of polarized measurements to aerosol absorption. We hope that our comments and modifications will fully answer to his questions and suggestions.

It has to be pointed out that some figures presented in this review are not in the manuscript as they only favor the understanding of specific questions of the reviewer.

General comments:

While the present work brings new information on the character of particles (SSA) of ACA scenes, I find a fundamental limitation of the POLDER approach presented in this paper. First, author retrieves scattering AOT on the basis of retrieved total AOT and assumed SSA using an algorithm developed by Waquet et al. (2008). The retrieved total AOT has been shown to be sensitive to the assumption of real and imaginary part of the refractive index (Table 1 in this manuscript). In the second step, the total radiance measurements and 'retrieved' scattering AOT was used to estimate the imaginary part of the refractive index and aerosol-corrected COT. In this way, the retrieval logic makes a full circle, i.e., starting with an assumption about SSA to retrieve total/scattering AOT and use the scattering AOT again to retrieve back SSA.

Actually, polarized radiances translate the scattering AOT. The method described in the study of Waquet et al. [2013] consists in the retrieval of the scattering AOT based on polarized measurements. Then, the total AOT is estimated using an assumption on the SSA. As stated in the section 2.1 of the manuscript, polarization is mostly sensitive to the first order of scattering. Also, in Fig. 2, one can see the weak contribution of the aerosol absorption to polarized radiances, especially at side scattering angle. This part of the signal (i.e. for scattering angle under 130°) is the one used in the polarized part of the retrieval for fine mode particles. In this way, the first step of the algorithm consists in the retrieval of the scattering AOT and the aerosol size from polarized radiances while the second part rests upon the adjustment of the absorption to fit the total radiance measurements.

Waquet, F., Cornet, C., Deuzé, J. L., Dubovik, O., Ducos, F., Goloub, P., Herman, M., Lapyonok, T., Labonnote, L., C., & Vanbauce, C. (2013). Retrieval of aerosol microphysical and optical properties above liquid clouds from POLDER/PARASOL polarization measurements. *Atmospheric Measurement Techniques*, 6(4), 991-1016.

In order to clarify this point, the section 2.3 of the manuscript has been corrected. In pages 25540-25541, lines 23 to 4 have been replaced by:

The retrieval of the scattering AOT is attempted for each $6\text{km} \times 6\text{km}$ POLDER's pixel when the COT given by MODIS is larger than 3.0. If fine mode aerosols have been identified, the estimation of the scattering AOT is based on the signal measured for scattering angle lower than 130° . At that point, a first estimation of the extinction AOT is made based on the absorption assumed for the selected aerosol model (i.e. $k_{\text{assumption}}$). Results are then subjected to several filters in order to improve their quality: data must be well fitted, clouds have to be homogeneous and both cloud edges and cirrus are rejected according to criteria based on POLDER and MODIS products. Filtered AOT are then aggregated from $6\text{ km} \times 6\text{ km}$ to $18\text{ km} \times 18\text{ km}$ and pixels with a Standard Deviation (SD) of the AOT larger than 0.1 are

excluded in order to prevent cloud edge contamination. Eventually, the scattering AOT is recovered using the SSA of the aerosol model with the same absorption assumption used at first (i.e. $k_{\text{assumption}}$):

$$\tau_{\text{scatt},\lambda} = \varpi_{0,\lambda,k_{\text{assumption}}} \tau_{\text{ext},\lambda,k_{\text{assumption}}} \quad (2)$$

Estimation of SSA of aerosols above cloud requires independent direct measurements of AOT such as from airborne sunphotometer or High Spectral Resolution Lidar (HSRL)-like extinction retrieval which are free from assumption about aerosol model.



Kaufman et al. have already shown that it is possible to retrieve aerosol SSA from passive measurements. He developed two methods to retrieve the aerosol absorption with passive satellite instruments. Both techniques rely on the attenuation of the signal above a bright surface. On the one hand, the first one (Kaufman, 1987; Kaufman et al., 2001) allows the evaluation of the SSA of dust aerosols above a bright surface as long as the scattering phase function and the surface reflectance are known (derived during a clear day for instance). On the other hand, Kaufman et al. (2002) suggest using the sunglint to retrieve the aerosol absorption above the ocean. The spectral contribution of the glint is derived from reflectance measured in a spectral band in which aerosols are transparent. In addition, the scattering properties of the aerosol layer, such as the scattering optical thickness and the size distribution, are retrieved with off-glint reflectances. Finally, the aerosol absorption is derived from the attenuation of the measurements acquired in the glint. In one sense, our method follows the same idea with the cloud used as a bright surface.

Kaufman, Y. J. (1987). Satellite sensing of aerosol absorption. *Journal of Geophysical Research: Atmospheres (1984–2012)*, 92(D4), 4307-4317.

Kaufman, Y. J., Tanré, D., Dubovik, O., Karnieli, A., & Remer, L. A. (2001). Absorption of sunlight by dust as inferred from satellite and ground-based remote sensing. *Geophysical Research Letters*, 28(8), 1479-1482.

Kaufman, Y. J., Martins, J. V., Remer, L. A., Schoeberl, M. R., & Yamasoe, M. A. (2002). Satellite retrieval of aerosol absorption over the oceans using sunglint. *Geophysical Research Letters*, 29(19), 34-1.

Author highlights in the paper that the uncertainty in scattering AOT can be greater due to wrong assumption of SSA for larger aerosol loading which is frequently observed over the south-eastern Atlantic Ocean. Under these circumstances, the reliability of SSA retrieval and further estimation of DRE is questionable. Additionally, the manuscript is devoid of an uncertainty analysis of SSA retrieval given the realistic bounds of error in the scattering AOT.

It is right that the approximation according to which polarized measurements only translate the scattering processes become less consistent when the aerosol layer is very absorbing (i.e. large AOT and low SSA). In order to qualitatively assess the impact of this approximation, we have made a statistical analysis of the events sampled in the middle of the fire season 2006 over the South-East Atlantic Ocean (August to September, 5°N to 30°S, 20°W to 20°E). This sample is expected to gather the most unfavorable cases for our algorithm since large amount of very absorbing aerosols are emitted during that period. The distribution of the AOT above clouds is presented in Fig. 1. Events with AOT lower than 0.2 at 865 nm constitute around

75% of the observed scenes. Then the distribution decreases dramatically with the AOT so that only 2.7% of events have an AOT larger than 0.4. This analysis confirms the validity of the approximation regarding polarized radiances for most cases.

In parallel, we have extended the sensitivity analysis of the manuscript to absorbing aerosol layer with increasing AOT. Aerosols with an effective radius of $0.1 \mu\text{m}$ have been considered with an imaginary part of the refractive index of 0.02 and 0.03, corresponding to a SSA at 865 nm of 0.836 and 0.772 respectively. The cloud used to model the signal has an optical thickness of 10.0 and a droplet effective radius of $10.0 \mu\text{m}$. Figure 2 shows the error on the retrieved SSA (i.e. $\Delta\text{SSA} = \text{SSA}_{\text{retrieved}} - \text{SSA}$) and the retrieved absorption AOT as a function of the AOT. For $\text{AOT} = 0.05$, the SSA is overestimated of about +0.036. The retrieved scattering AOT with polarization is correct but the aerosol size is slightly overestimated ($0.12 \mu\text{m}$ instead of $0.10 \mu\text{m}$). When the aerosol layer is thicker, the SSA is always underestimated. For $\text{AOT} = 0.2$, we observe a bias of -0.017 and -0.029 for SSA equal to 0.836 and 0.772 respectively. In case of an extreme event with AOT around 0.5 at 865 nm (i.e. 1.3 at 550 nm), the bias is valued at -0.055 for $\text{SSA} = 0.772$. However, it has to be pointed out that the underestimation of the SSA always goes together with an underestimation of the scattering AOT. Because total radiances are sensitive to the absorption of the aerosol layer, the algorithm compensates the error on the scattering AOT due to the first part of the retrieval by an underestimation of the SSA. The absorption AOT is thus less impacted by the approximation on polarized radiances than the SSA. According to Eq. (1) in the manuscript, the absorption AOT is the leading parameter in the estimation of the DRE for large values of the underneath surface albedo. Figure 1 is not shown in the manuscript to keep the general character of the sensitivity analysis and for now on, Fig. 2 is a part of the new Fig. 5.

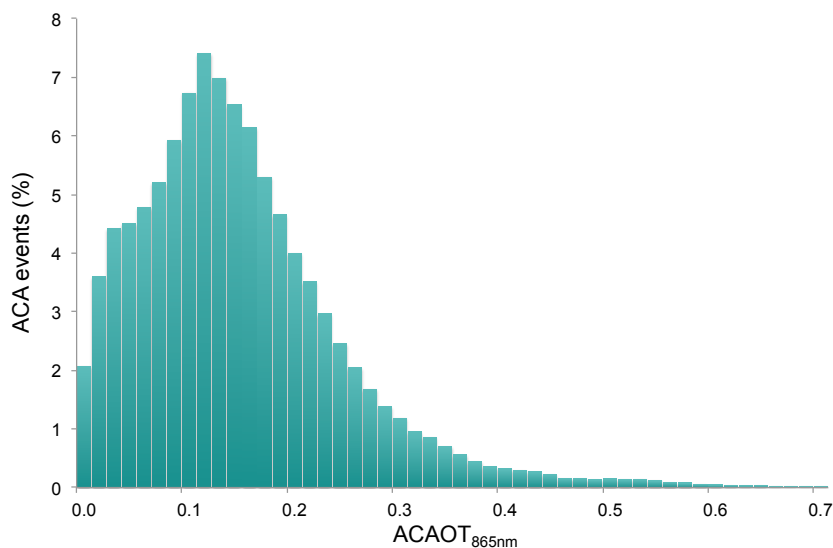


Figure 1. Distribution of the Above Cloud Aerosol Optical Thickness at 865 nm ($\text{ACAOT}_{865\text{nm}}$) from August to September 2006 over the South-East Atlantic Ocean (5°N to 30°S , 20°W to 20°E).

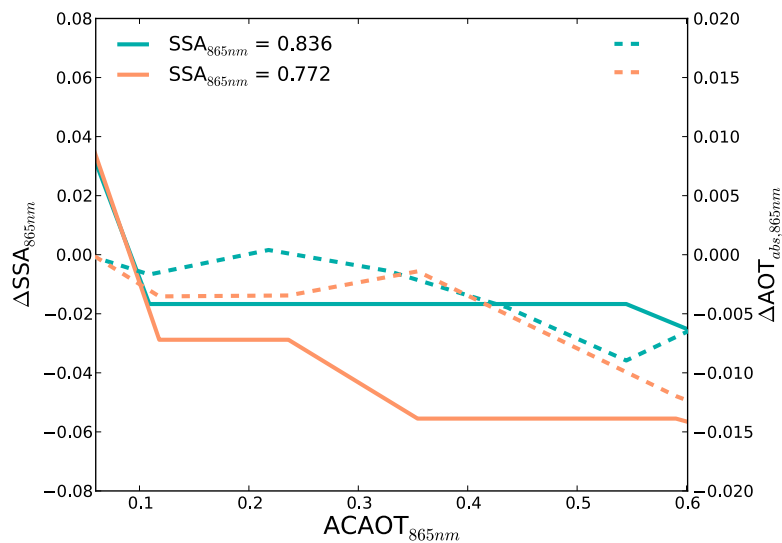


Figure 2. Error in the retrieval of the SSA (i.e. $\Delta\text{SSA} = \text{SSA}_{\text{retrieved}} - \text{SSA}$; solid lines) and the absorption AOT (i.e. $\Delta\text{AOT}_{\text{abs}} = \text{AOT}_{\text{abs, retrieved}} - \text{AOT}_{\text{abs}}$; dashed lines) as a function of the Above Cloud AOT at 865 nm for aerosols with SSA of 0.836 and 0.772 (green and orange lines respectively).

The sensitivity analysis in section 2.4 has been modified (see Specific comments).

Specific comments:

Page 25534, Line 2: While most satellite retrievals of above cloud aerosols...

The beginning of the abstract has been rephrase:

This study presents an original method to evaluate key parameters for the estimation of the direct radiative effect of aerosol above clouds: the absorption of the aerosol layer and the albedo of the underneath cloud.

Page 25534, Line 19: +33.5 W/m² (warming)

The clarification has been added to the manuscript, thank you.

Page 25535, Line 11: Since the DELTA_RHO is a strong function of AOD and SSA of aerosols above cloud, adding the simulation for SSA of 0.9 would highlight the sensitivity of TOA reflectance to the aerosol SSA. What is the value of AOD assumed for this simulation? Since the interest here is to estimate aerosol forcing above cloud, a similar plot as a function of cloud optical depth is desirable.

Lines corresponding to SSA of 0.9 have been added to Fig. 1 of the manuscript. The simulations processed for this figure are independent from the AOT since the horizontal axis represents the ratio of the albedo difference on the AOT.

Although we are interested in aerosol forcing above cloud, we have chosen not to plot the Fig. 1 as a function of the Cloud Optical Thickness (COT) in order to preserve the qualitative and general scope of this analysis. Moreover, the albedo of a cloud depends not only on the COT

but also on the solar zenith angle and the wavelength. The simulations used to plot the figure have been made by considering single values of the SSA and g . Using a realistic cloud as the underneath surface would require to spectrally integrate the albedo of the scene and consequently, to consider the spectral variation of the aerosol properties.

Page 25535, Line 19: contribution instead of importance

Page 25537, Line 6: Jethva et al. (2014) have carried out a multi-sensor comparison of the above-cloud AOT retrieved from different sensors on board NASA's A-train satellite.

Page 25537, Line 8: "...results have shown good consistency over the homogeneous cloud fields".

These sentences have been corrected as suggested by the reviewer.

Page 25537, Line 20: While this method is expected to work efficiently for the fine mode aerosols as their interactions at longer wavelengths are minimal or even nil. it may not work for coarse mode dust aerosols due to their radiative interference at longer wavelengths.

The sentence has been rectified in accordance with the reviewer proposition (expect for the word "interference" that has been replaced by "influence").

Page 25541, Eq 2: Here, I have a fundamental question to the author: First, the POLDER retrieval algorithm retrieves total AOT assuming a model with a fixed value of SSA. What is the sensitivity of the AOT retrieval to the assumed value of SSA? Figure 2 has demonstrated the sensitivity of polarized radiances to the imaginary index around the scattering range angle 140-145 deg.

The answer to this question is partly given in the general comment response and the manuscript has been edited accordingly. Regarding the sensitivity of polarized radiances to aerosol absorption in the cloud bow (i.e. for scattering angle around 140°), it has to be noticed that this part of the signal is not used to retrieve the scattering AOT for fine mode aerosols. As mentioned in Waquet et al. (2013), the algorithm does the discrimination between the fine mode and dust in the first place. When fine mode aerosols are detected, only the polarized signal measured for scattering angles lower than 130° is used to retrieve the scattering AOT. For dust particles, the whole signal is used to retrieve the scattering AOT. However, the assumption on the absorption of dust at 865 nm is the same in the polarized and the total radiance part of the retrieval.



Waquet, F., Cornet, C., Deuzé, J.-L., Dubovik, O., Ducos, F., Goloub, P., Herman, M., Lapyonok, T., Labonnote, L. C., Riedi, J., Tanré, D., Thieuleux, F., and Vanbauce, C.: Retrieval of aerosol microphysical and optical properties above liquid clouds from POLDER/PARASOL polarization measurements, *Atmos. Meas. Tech.*, 6, 991–1016, doi:10.5194/amt-6-991-2013, 2013.

Page 25541, Line 25: provide an appropriate citation.

The reference to the paper of Rossow et al. [1989] has been added.

Rossow, W. B., Garder, L. C., and Lacis, A. A.: Global, seasonal cloud variations from satellite radiance measurements, Part I: Sensitivity of analysis, *J. Climate*, 2, 419–458, 1989.

Page 25541, Line 27: Do author retrieve ACAOT over sun-glint areas?

Yes, we retrieve the ACAOT over sun-glint areas since we take into account the reflectance of the ocean as a function of the wind speed. The uncertainty regarding the wind speed estimation should impact weakly the reflectance owing to the attenuation of the signal caused by the cloud layer.

Page 25542, Line 15: Where is the UV wavelength in Figure 4? I can see 490 nm (visible) and 865 nm (SWIR) in this figure.

The denomination UV has been changed by visible line 15 and line 18.

Page 25542, Line 18-19: This is called the 'color ratio' effect. Since aerosol absorption has a spectral signature, it produces stronger absorption effects at shorter wavelengths than at longer ones.

The sentence has been rephrased to include this specification:

However, one can notice the increasing gap between visible and SWIR radiances as the absorption grows called the color ratio effect. Since aerosol absorption has a spectral signature, it produces stronger absorption effects at shorter wavelengths than at longer ones.

Page 25543, Line 1-5: What is the SSA for the reference case?

The SSA for the reference case is equal to 0.911 at 865 nm.

Page 25543, Line 13: Author should list the % change in AOT and SSA retrieval in Table 3. It is easier to understand.

Page 25543, Line 20: The climatological value of SSA at 865 for the AERONET station 'Mongu' situated in the central Africa region is about 0.78. The ratio of AOT between 865 and 500 nm for the biomass burning season (July through September) is about 0.35. During active burning period the AOD at 500 nm often exceeds a value of unity. Under these high aerosol loading conditions, the wrong assumptions of both real and imaginary part of the refractive index will lead to significant error in the retrieval of scattering AOD and then in the SSA estimation using the present method. Also, it is desirable to have a simulation in which the real as well as imaginary part of the refractive index go wrong in such a way that it results in the total error in scattering AOT and SSA. This will give an estimation of the bounds of errors. Author should also mention here that though the retrieval of AOT is less sensitive to the assumption of imaginary part of the refractive index, the error is much larger due to wrong assumption of the real part of the refractive index.

Page 25543, Line 24: how the dust retrievals are impacted by assumption of real and imaginary part of the refractive index? A sensitivity analysis, similar to smoke particles, is needed here.

For the sake of clarity, the sensitivity analysis has been extended and the whole section 2.4 has been replaced by:

The method developed hereinbefore requires assumptions at different stages of the retrieval. The aim of this section is to analyze the resulting impact on the retrieval. To serve this purpose, POLDER's observations have been modeled with the same radiative transfer code used for the LUT, considering several aerosol and cloud models. Errors due to the polarization part of the retrieval are investigated and then, impacted on the total radiances step.

We first examine the assumption regarding aerosol properties. In order to retrieve the scattering AOT, it is assumed that polarized measurements are weakly sensitive to aerosol absorption. This approximation is expected to become less consistent when the aerosol layer is very absorbing (i.e. large AOT and low SSA). This leads to an error in the estimation of the scattering AOT that could affect the retrieval of the SSA. The second assumption concerns the real part of the refractive index m fixed at 1.47 for the retrieval. To assess the impact of these assumptions, we have considered 3 absorbing aerosol models with different refractive indices n : $1.42 - 0.03i$, $1.47 - 0.03i$ and $1.52 - 0.03i$ corresponding to a SSA at 865 nm of 0.735, 0.772 and 0.801, respectively. The real parts of the refractive indices have been chosen to be representative of the variability observed within the aerosol fine mode [Dubovik et al., 2002]. Aerosols have an effective radius of $0.1 \mu\text{m}$ and their mean altitude is 3 km. The cloud layer used to model the signal has a top altitude at 0.75 km, an optical thickness of 10 and a droplet effective radius of $10 \mu\text{m}$. Total and polarized radiances have been simulated for absorbing aerosol layers with increasing AOT. Finally, the DRE of aerosols has been processed using the radiative transfer code GAME [Dubuisson et al, 2004], based on the properties of the modeled scene on the one hand, and those retrieved by the algorithm on the other hand. In Fig. 5, the aerosol and cloud parameters retrieved (green lines) and used in the input simulations (grey lines) are plotted as a function of the AOT at 865 nm. The middle column (i.e. $n = 1.47 - 0.03i$) shows the biases due to the approximation that polarized radiances translate the scattering process only while the left and the right ones (i.e. $n = 1.42 - 0.03i$ and $1.52 - 0.03i$) present also the effect due to the assumption on the real part of the refractive index.

- The first two rows display the total and the scattering AOT. For $m = 1.42$ and 1.47 , the algorithm underestimates the AOT. This error comes from the underestimation of the scattering AOT during the polarized part of the retrieval. For AOT lower than 0.2, we observe a bias around 20% on the AOT. In case of extreme events, with AOT around 0.6 (i.e. 1.5 at 550 nm), the AOT is underestimated of 26.7% for $m = 1.47$ and 24.1% for $m = 1.42$, respectively. On the opposite, the algorithm overestimate the AOT when $m = 1.52$. It has to be noted that the retrieved aerosol radius is larger than the one use to model the signal ($0.12 \mu\text{m}$ instead of $0.1 \mu\text{m}$). In that case, the largest error on the AOT (i.e. 25.3%) is observed at AOT = 0.2. Then, the error slowly decreases with the AOT because of the compensation with the aerosol absorption, reaching 16.8% at AOT = 0.6.


- Rows 3 and 4 of Fig. 5 show the absorption AOT and the SSA versus the total AOT. In spite of the error on the scattering AOT, it is interesting to observe that the biases on the absorption AOT are small. Because of the sensitivity of total radiances to the absorption of the aerosol layer, the algorithm compensates the bias on the scattering AOT due to the first part by an error on the SSA. As a consequence, a negative error (resp. positive) in the scattering AOT goes together with an underestimation (resp. overestimation) of the SSA. For AOT = 0.6, a bias of -0.055 has been observed for $m = 1.42$ and 1.47 and $+0.033$ for $m = 1.52$, respectively.



- Plots of the 4th row represent the retrieved COT. They reveal that both the approximation regarding polarized radiance and the assumption on the real part of the refractive index have a limited impact on the COT estimation. In this analysis, the largest bias is ± 0.3 on the COT.

- Finally, the last row focuses on the evolution of the DRE of aerosols with the modeled AOT. The DRE estimated with aerosol and cloud properties retrieved by the algorithm is close to the one processed with the properties of the modeled scene. This can be explained by the reliable estimation of the aerosol layer absorption: as suggested by Eq. (1), the absorption AOT is the leading parameter in the estimation of the DRE for large values of the albedo of the underneath scene. The largest bias ($+9.7 \text{ W.m}^{-2}$) has been obtained for $\text{AOT} = 0.6$ and $m = 1.52$. Otherwise, the bias is always lower than $\pm 6.4 \text{ W.m}^{-2}$ for AOT lower than 0.2 and lower than $\pm 1 \text{ W.m}^{-2}$ for AOT lower than 0.1.

In a second place, we look at the assumption on the size distribution of the coarse mode particles. For the retrieval, we only consider one model for dust. It is defined by a bimodal lognormal size distribution with an angström exponent of 0.36 [Waquet et al., 2013a]. The signal has been modeled for coarse mode particles with an angström exponent of 0.02 and 0.6 and an $\text{AOT} = 0.6$. The method appears to allow a consistent evaluation of the SSA at 490 nm (error $< 1\%$) in spite of the error on the optical thickness and on the angström exponent (error on AOT around 24% and on angström exponent 100%).

The last assumption about aerosols that has been investigated concerns the vertical distribution of the aerosol layer. We have processed the signal for an aerosol top altitude of 4 and 6 km and the algorithm has retrieved the correct aerosol and cloud properties. In polarization, the bands used to retrieve the scattering AOT (i.e. 670 and 865 nm) are weakly impacted by the molecular contribution. Aerosols in the clouds do not contribute to the creation of polarized signal at side scattering angle. Hence the polarized radiances are not impacted by the aerosol vertical distribution as long as the aerosol layer is distinct from the cloud. 

Regarding the cloud hypothesis, we test the impact of considering only one cloud droplet effective radius ($r_{\text{eff,clد}} = 10 \mu\text{m}$) for the estimation of the aerosol absorption and the ACCOT by modeling the signal for $r_{\text{eff,clد}} = 6$ and $20 \mu\text{m}$ with a $\text{COT} = 10$. The approximation regarding the effective radius of cloud droplet is the main source of error on the COT estimation. While the error on the COT due to aerosol hypothesis does not exceed 3%, this one may lead to a bias of $\pm 10\%$ for the COT, which is in agreement with the study of Rossow et al. [1989]. However, statistical analysis of the scenes studied hereafter have shown that more than 70% of the clouds have an effective radius ranging between 8 and $16 \mu\text{m}$. Lastly, we have investigated the influence of the cloud top altitude by considering $z_{\text{top,clد}} = 2$ and 4 km. For each case, the algorithm has retrieved the correct parameters for clouds and aerosols.

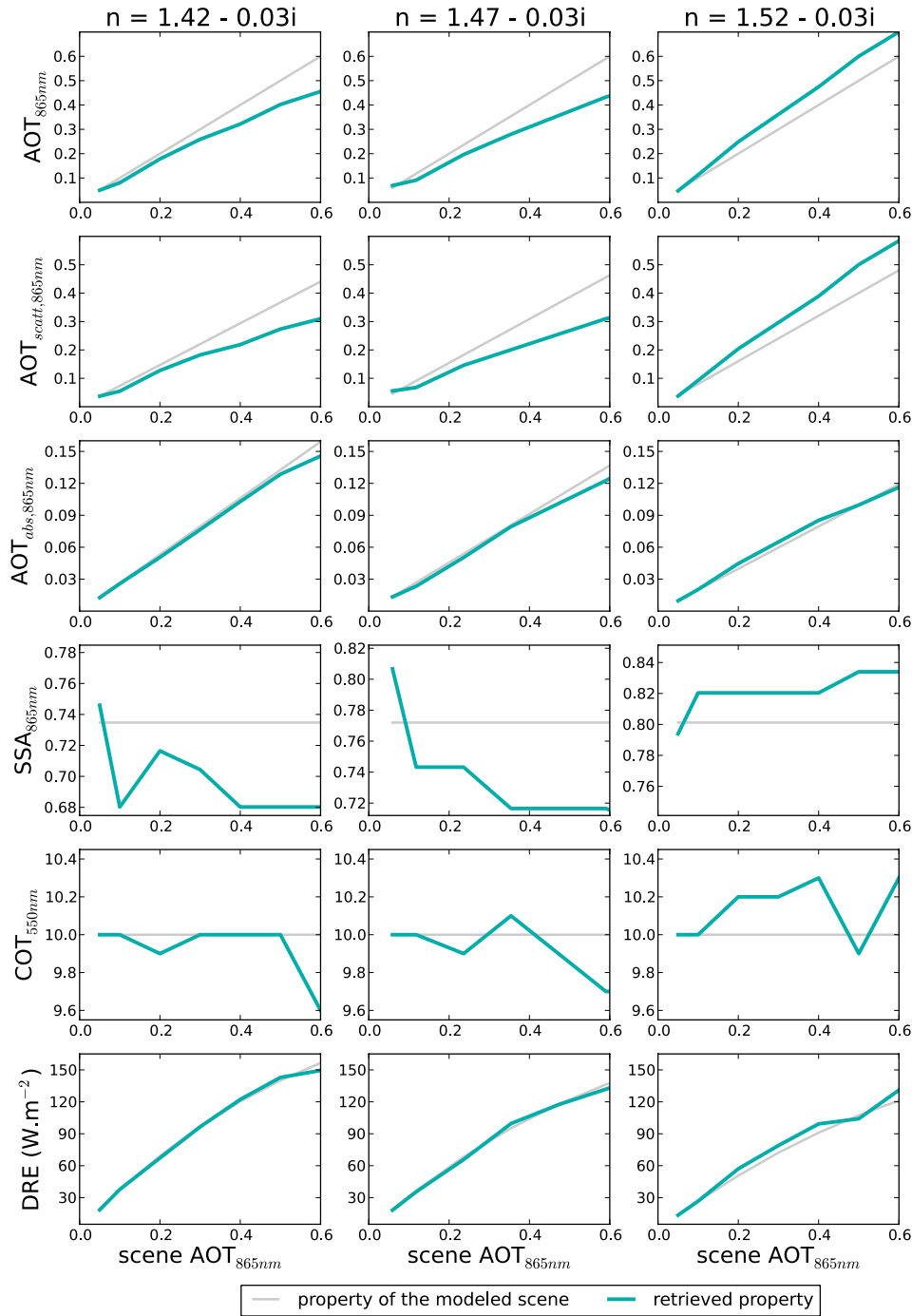


Figure 5. Sensitivity of the retrieved properties of an AAC scene with different aerosol models. From top to the bottom: total AOT, scattering AOT, absorption AOT and SSA at 865 nm, COT at 550 nm and the short wave DRE of aerosols. Grey lines correspond to the properties of the actual modeled scene and green lines to those retrieved by the algorithm. The aerosol model of the first column has a refractive index n equal to $1.42 - 0.03i$, the second, $n = 1.47 - 0.03i$ and the third, $n = 1.52 - 0.03i$. Aerosols have an effective radius of $0.1 \mu\text{m}$ and the effective radius of the cloud water droplets is $10 \mu\text{m}$.

Page 25545, Line 7: What is the range of wavelengths considered as 'shortwave'?

The solar fluxes are integrated from 200 nm to $4 \mu\text{m}$. This information has been registered in the manuscript page 25545 line 7:

Instantaneous shortwave radiative forcing (i.e. from 0.2 to 4 μm) has been precomputed for several solar zenith angles.

Page 25545, Line 9: It implies that author assumes 'grey aerosols' for the DRE calculation. For smoke particles, it means that the black carbon is assumed to be a sole component of carbonaceous aerosols.

The sentence page 25545 lines 8-10 has been modified to include this clarification:

Regarding fine mode aerosols, they are assumed to be only composed of black carbon. In other words, the imaginary part of the refractive index is constant in the shortwave (grey aerosols) and corresponds to the one retrieved by our algorithm.

Page 25545, Line 23: "...weakly impacted by the change in cloud top height"?

In the paper of Waquet et al. [2009], the cloud top heights retrieved by several methods (i.e. MODIS IR technique, [Menzel et al., 2006], POLDER Rayleigh [Goloub et al., 1994] and POLDER O₂ [Vanbauce et al., 2003] techniques) are shown together with CALIOP observations for an aerosol above cloud scene. This comparison reveal that aerosols above clouds highly disrupt the retrieval of the cloud top height by the IR and the Rayleigh methods while the values retrieved with the O₂ method remain close to the CALIOP observations (accuracy of ± 350 m for the case study). The sentence page 25545 lines 21-23 has been rephrased:

The cloud top height is derived from the POLDER apparent O₂ cloud top pressure [Vanbauce et al., 2003] since the O₂ retrieval allows a reliable estimation of the cloud top height in the presence of an aerosol layer above [Waquet et al., 2009].

Goloub, P., J.-L. Deuzé, M. Herman, and Y. Fouquart (1994), Analysis of the POLDER polarization measurements performed over cloud covers, IEEE Trans. Geosci. Remote Sens., 32, 78–88.

Menzel, W. P., R. A. Frey, B. A. Baum, and H. Zhang (2006), Cloud Top Properties and Cloud Phase Algorithm Theoretical Basis Document, Version 7, 55 pp. [Available online at: <http://modisatmos.gsfc.nasa.gov/docs/MOD06CT:MYD06CTATBDC005.pdf>, last access: August 2012].

Vanbauce, C., B. Cadet, and R. T. Marchand (2003), Comparison of POLDER apparent and corrected oxygen pressure to ARM/MMCR cloud boundary pressures, Geophys. Res. Lett., 30(5), 1212, doi:10.1029/2002GL016449.

Waquet, F., J. Riedi, L. C. Labonnote, P. Goloub, B. Cairns, J.-L. Deuzé, and D. Tanré (2009), Aerosol remote sensing over clouds using the A-Train observations, J. Atmos. Sci., 66, 2468–2480, doi:10.1175/2009JAS3026.1.

Page 25546, Line 1: Either rephrase or remove this sentence.

The sentence has been removed.

Page 25546, Line 13: It is winds that favor the transport of smoke over ocean and not stratocumulus cover.

The sentences page 25546 line 11-14 have been rephrased:

From June to October, biomass burning particles from man made vegetation fires are frequently observed above the persistent deck of stratocumulus covers off the South West African coast.

Page 25547, Line 2: Did author check the value of SSA (870 nm) retrieved by AERONET at Mongu-an inland station for the Aug 4, 2008 time frame?

On 4th August 2008, the SSA retrieved by AERONET at Mongu station is 0.716 at 870 nm, which is larger than the value observed for that case study (averaged value of 0.840 and minimum value of 0.73 near the coast). Also, the angström exponent at the inland site is found to be larger than the one observed with POLDER (2.19 for AERONET against 1.94 over the scene) that may be due to the increasing of the aerosol size during its transport. Sayer et al. [2014] have already notice larger value of the aerosol radius between Mongu and Ascension Island. This AERONET station is closer to our case study but no measurements are available in that time frame. Although, the study of Sayer et al. [2014] also notes that the SSA values retrieved at Ascension Island range from 0.73 and 0.83 at 870 nm, which supports POLDER's results. The reference to this paper has been added page 25547 line 3 as well as Johnson et al. [2008] line 4.



Johnson, B. T., Osborne, S. R., Haywood, J. M., & Harrison, M. A. J. (2008). Aircraft measurements of biomass burning aerosol over West Africa during DABEX. *Journal of Geophysical Research: Atmospheres (1984–2012)*, 113(D23).

Sayer, A. M., Hsu, N. C., Eck, T. F., Smirnov, A., & Holben, B. N. (2014). AERONET-based models of smoke-dominated aerosol near source regions and transported over oceans, and implications for satellite retrievals of aerosol optical depth. *Atmospheric Chemistry and Physics*, 14(20), 11493-11523.

Page 25547, 2nd paragraph: The absolute difference between two COTs does not tell the full story. A plot of % change in COT (ACCOT minus MODIS MYD06 COT) as a function of retrieved AOT would explain how the absorption is impacting the standard MODIS cloud product.

Figure 3 deals with the relative difference between POLDER ACCOT and the MODIS COT as a function of the absorption AOT. As expected, the bias increases with the absorption AOT. Also, we can see the large negative differences at low absorption values. For clouds with a small optical thickness (i.e. lower than 7), the scattering due to the aerosol layer may lead to a brighter scene. However, POLDER and MODIS are different by nature (different instruments and assumptions for the COT retrieval). For clean-sky, differences have been observed between the POLDER and the MODIS estimation of the COT [Zeng et al., 2012]. Even in case of very low aerosol content, we do not expect a perfect consistency between the two COT estimations. Consequently, Fig. 3 does not only translate the impact of aerosol absorption on the COT retrieval.



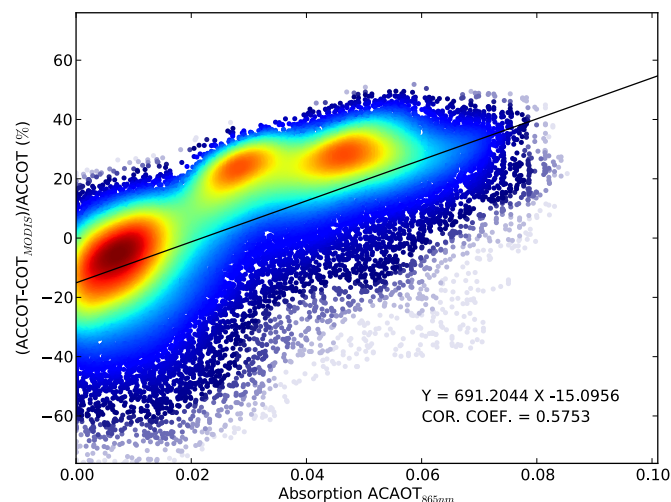


Figure 3. Relative difference between POLDER AACOT and MODIS COT as a function of the absorption AOT above clouds for biomass burning aerosol the 4th August 2008.

Zeng, S., C. Cornet, F. Parol, J. Riedi, and F. Thieuleux (2012). A better understanding of cloud optical thickness derived from the passive sensors MODIS/AQUA and POLDER/PARASOL in the A-T rain constellation, *Atmos. Chem. Phys.*, 12, 11245–11259, doi:10.5194/acp-12- 30 11245-2012.

Page 25548, Line 5: "...significant production of smoke particles".

Page 25548, Lin8: "On 3rd July, aerosols have been..."

These corrections have been made, thank you.

Page 25548, Line 15: Did author compare MODIS cloud-free ocean retrieval nearby above-cloud aerosols retrieved by POLDER. Since the smoke plume is lofted well above the surface, both retrievals should provide consistent range of AOT retrievals over ocean.

We have chosen to carry out the comparison with cloud-free AOTs retrieved with measurements with the same instrument. A new algorithm to retrieve aerosol properties (AOT, angström exponent, SSA ...) in clear-sky scenes with POLDER is under development. The AOT retrieved with both methods has been compared for the Siberian biomass burning episode on 3rd July (Fig. 3) and for dust event on 4th August (Fig. 4). The continuity between the two retrievals shows a good consistency over ocean. The new POLDER approach over clear-sky will be the subject of an upcoming publication together with a comparison analysis with the above cloud results.

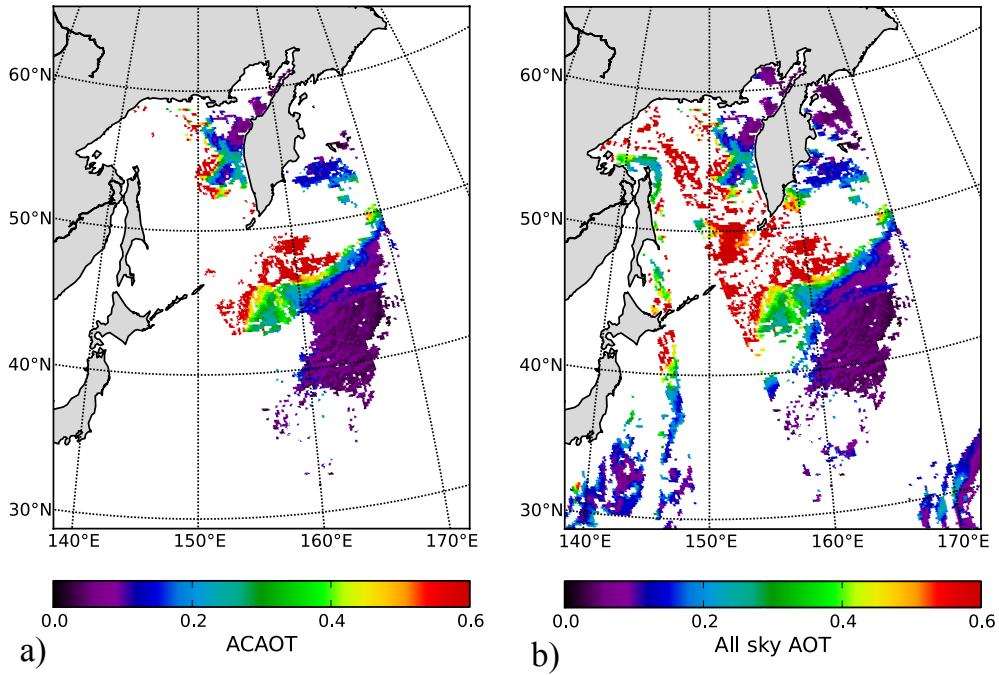


Figure 4. Above clouds (a) and all sky (b) AOT at 865 nm retrieved with POLDER for biomass burning aerosols from Siberia the 3 July 2008.

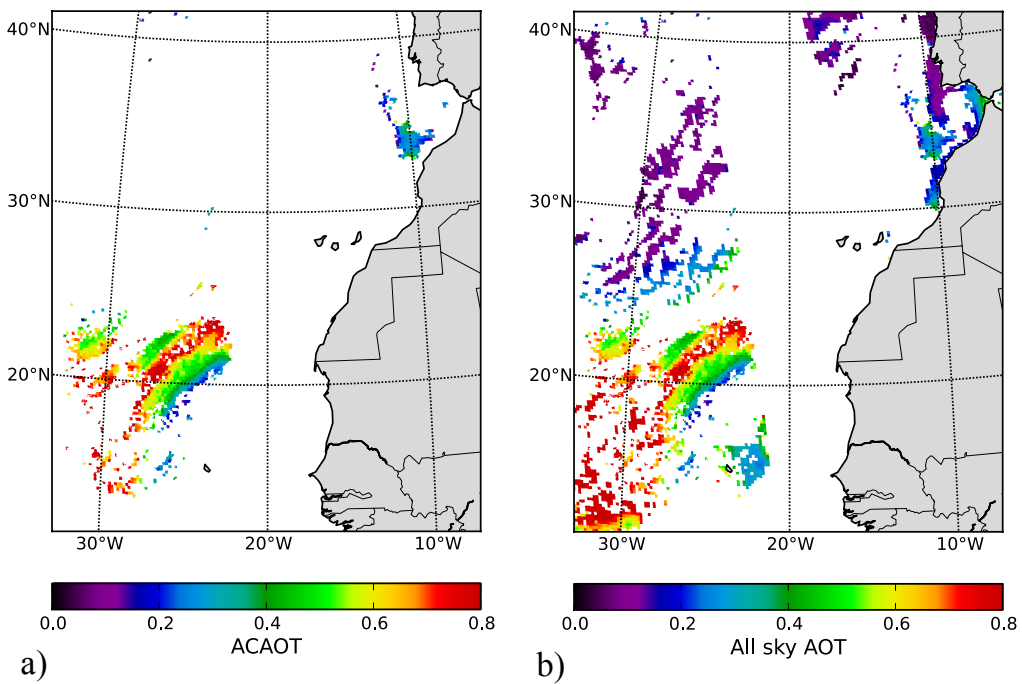


Figure 5. Same as Fig. 3 for the dust event the 4 August 2008.

Page 25550, Line 1: "in the visible (490 nm)"

The sentence has been corrected, thank you.

Page 25550, 1st paragraph: Again, author should check what MODIS retrieves over the clear ocean and what AERONET provides in terms of SSA at stations around the source region.

The SSA values obtained at the AERONET station at Tenerife are 0.936 and 0.969 at 490 (interpolated value) and 870 nm, respectively. These estimations are close to the POLDER ones in the southern part of the scene (i.e. 0.947 at 490 nm and 0.965 at 865 nm). However, comparisons between above cloud and clear-sky retrievals have to be considered carefully because of potential contamination of low-level aerosols.

Page 25551, Line 19-20: This is very much consistent with the results of de Graaf et al. (2012)

The reference has been added to the manuscript.

Page 25552, Line 14: What is the minimum value of COT considered in the estimation of DRE?

The minimum value considered for the COT is 3. This clarification is now mentioned in the manuscript.

Page 25555, section 6: A brief discussion on the uncertainty bounds of the AOT and SSA retrieval, and then after on DRE estimation, is missing in the conclusion section. This discussion should highlight the strength and limitation of the present approach.

The following paragraph has been added page 25555, line 20:

Nevertheless, the impact of the approximations and the assumptions of the method have been assessed. The largest uncertainty about the SSA is due to the approximation about the weak sensitivity of polarized radiances to absorption. When the aerosol size distribution is dominated by the fine mode, an underestimation of -0.055 can be expected for extreme event of absorbing aerosols above clouds (i.e. $AOT_{865nm} = 0.6$ and $SSA_{865nm} = 0.77$). Otherwise, the bias on the SSA is below 0.03. It has to be pointed out that the underestimation of the SSA always goes together with an underestimation of the scattering AOT. As a consequence, the algorithm presented here provides a reliable estimation of the absorption AOT, which is among the most important parameters to evaluate the DRE of aerosols above clouds.

Page 25555, Line 20-21: Author needs to be little more cautious here. Before these retrievals are validated against independent direct measurements of AOT above cloud, one cannot arrive at a conclusion about the accuracy of the satellite product.

“Accurately” has been removed from this sentence.

We are thankful to the anonymous reviewer for her/his help in improving the quality of this manuscript. Please, find below our answer to your question and commentaries.

Let us mentioned that some plots in this document have not been included in the new version of the manuscript when they only illustrate a specific answer to the reviewer question.

Main comments:

(1) It should be mentioned clearly in the abstract and the conclusions that the results presented here are only valid for $COT > 3$. Since DRE is highly dependent on COT, cloud albedo and cloud fraction, this selection criterion automatically generates DRE that are biased high, since many negative and low values are not considered.

The abstract and the conclusion now mention the information about the selection of the scene. Thank you for the suggestion:

Page 25534 line 14: The retrieval of aerosol and clouds properties (i.e. aerosol and cloud optical thickness, aerosol single scattering albedo and angström exponent) is restricted to homogeneous and optically thick clouds (cloud optical thickness larger than 3).

Page 25555 line 10: Its range of application is restricted to homogeneous cloud with COT larger than 3.

Page 25556 line 24: Let us point out that differences between the result of this study and the literature are expected and are mainly due to the selection of the AAC scenes: this analysis does not include thin clouds (i.e. $COT < 3$) and scene with fractional cloud coverage which leads to biased high the DRE.

(2) 2.4 Sensitivity analysis (25542-25544) This is the weakest part of the paper. Some hints are given as to how the algorithm behaves in a few cases, but no clear picture is given of how sensitive the algorithm actually is under different circumstances. A few results are given in tables, but pictures showing the various limitations and sensitivities would be much more helpful. This should be incorporated in this paper, as this paper presents the applicability of the polarization measurements for the computation of the DRE. To assess the uncertainty of the DRE results it is necessary to understand the sensitivity of the retrievals of the aerosol and cloud parameters. The lack of this sensitivity study is most clearly indicated by the following sentences: Lines 21-23: " Of course, we expect larger biases for larger AOT. However, the quantity of aerosols chosen to process the synthetic radiances is representative of the ACA events that have been already observed in Waquet et al. (2013b)." The range of 'quantity' given in table 3 is $AOT=0.12$ to $AOT=0.2$. Even in the present manuscript the range in AOT is much larger than that. It should be clear what happens to the accuracy of the retrievals in those cases.

Similarly, the last paragraph (lines 25544, 7-17) signal a very important uncertainty, which will impact the DRE results dramatically. Showing only two points is not very adequate. Do the results respond linearly to the bias? And 70% falls within 8-16 microns, but the remaining 30% will provide the extreme values that are presented in the manuscript. Are they reliable?

These issues should be addressed in a sensitivity analysis that shows the most important relationships between the algorithm assumptions, the retrieved parameters and the resulting DRE.

The sensitivity analysis in section 2.4 has been entirely revised. The impact of the approximation according to which polarized radiances translate only scattering processes has been assessed together with the assumption on the real part of the refractive index. This analysis has been performed in terms of biases on both retrieved properties and DRE estimation. This section also includes sensitivity tests about the coarse mode size distribution and refractive index.

Regarding the extreme values of the DRE, we have plotted the distribution of the DRE of aerosols above clouds as a function of the cloud droplet effective radius for the African biomass burning event the 4 August 2008 (Fig. 1). No correlation is observed between these two parameters. Moreover, the extreme DRE are obtained for cloud droplet effective radius between 10 μm and 12 μm .

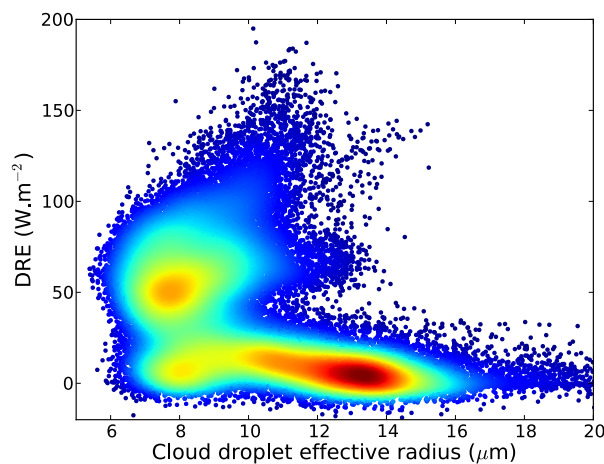


Figure 1. Distribution of the aerosol above cloud DRE as a function of the cloud droplet effective radius for the African biomass burning event off the Namibian coast, 4th August 2008.

(3) Figures 6,7, and 8 -In all these figures the scales of the plotted quantities do not match the description in the text! Apparently the ranges have been cut at a certain maximum, but this is not clear in the picture. This should be corrected. If the authors prefer to show only a part of the whole range, than the color bars should be annotated indicating that the range was cut. E.g. 6a: 0.0, 0.1, 0.2, >=0.3. The figures should be clear by themselves, and not only after a thorough (and confusing) read of the text. Since all three figures were created like this, as I understand after reading the text, I urge the authors to reconsider all figures to make sure this is corrected in all of them. -The captions are too short and too general. All 6 panels should be described in the caption, so that the figures make sense without a thorough read through the text. -The colorbar annotations are illegible.

Figures 6, 7 and 8 (for now on, 7, 8 and 9) has been modified to make clear that some colorbars are saturated and to make legible the annotations. The descriptions of the 6 plots have been added to the caption of Fig. 7:

Figure 7. Biomass burning aerosols above clouds off the South West African Coast the 4 August 2008. The panel displays the Above Cloud AOT at 865 nm (a), the Angström Exponent (b), the aerosol SSA at 865 nm (c), the Aerosol Corrected COT at 550 nm (d), the difference Δ COT of the AACOT and the MODIS COT (e) and the Direct Radiative Effect of aerosols above clouds in $W.m^{-2}$ (f).

(4) In all experiments the used parameters should be mentioned and presented, e.g. in tables.

Textual comments:

Abstract

lines 2-7: "While most of the retrievals of above clouds aerosol characteristics rely on assumptions on the aerosol properties, this study offers a new method to evaluate aerosol and cloud optical properties simultaneously (i.e. aerosol and cloud optical thickness, aerosol single scattering albedo and angström exponent)". The word 'while' implies that this is not true for his method. However, the method presented here still relies on the correct selection of aerosol models through use of an inversion method, and is essentially not different from most other methods. However, since more independent information is used, the selection of the aerosol properties can be better constrained. Please, rephrase.

The beginning of the abstract has been rephrased:

This study presents an original method to evaluate key parameters for the estimation of the direct radiative effect of aerosol above clouds: the absorption of the aerosol layer and the albedo of the underneath cloud.

line 15: '...based on exact modeling.' The authors mean 'exact' here as opposed to the approximate method of eq. 1. However, this is not clear here in the abstract without the context. Obviously, one would use an exact (as possible) method to compute something. This should be rephrased to indicate which exact and approximate methods are meant. Or just removed.

This part has been removed.

line 15-16: Similarly: "beside THE three case studies..". These three case studies have not been introduced at this stage, so describe more generally in the abstract what the paper is about.

A brief description of the case studies have been added to the abstract:

Three case studies have been selected: a case of absorbing biomass burning aerosols above clouds over the South-East Atlantic Ocean, a Siberian biomass burning event and a layer of Saharan dust above clouds off the North-West African coast.

lines 19-24: In my opinion, the result that cloud heterogeneity of clouds "leads to a slight underestimation" of the DRE is a very important result. It has become clear that highly models underestimate the DRE of ACA, and most analyses indicate that cloud brightness/fraction is probably the culprit, since it has such a strong influence on the resulting DRE. Heterogeneity also has an important effect, as shown here: 10% underestimation for an inhomogeneity parameter of 0.6. To me, 10% is a serious effect, the authors claim that an inhomogeneity parameter of 0.6 represents a normal value for stratocumulus clouds. This effect should be investigated further, and the authors should present a sensitivity analysis of the inhomogeneity of clouds on the DRE of ACA. That would present a real new addition to this scientific field.

Not taking into account the cloud heterogeneity in the retrieval and the processing of the DRE leads to biases in the evaluation of the DRE of aerosols above clouds. We agree that a study of the impact of cloud heterogeneity on the estimation of the DRE would be very useful. However, 3-D radiative transfer simulations are time-consuming (especially for spectrally integrated fluxes) and a complete analysis of this effect would require a separate study. Also, as mentioned, from now on, in section 2.3, the retrieval of aerosol and cloud properties is only attempted for relatively homogeneous clouds (filter based on MODIS product). We expect to have the highest DRE (and thus, the largest biases) over the South East Atlantic Ocean during the fire season. A statistical analysis has been performed from June to August 2008 over this area. Figure 2 shows the distribution of the heterogeneity parameter ρ for ACA events selected by the algorithm. Only 5% of events have a heterogeneity parameter larger than 0.45 and it is lower than 0.3 for 73% of these ACA scenes. For this reason, we expect a limited impact of cloud inhomogeneity in this study.

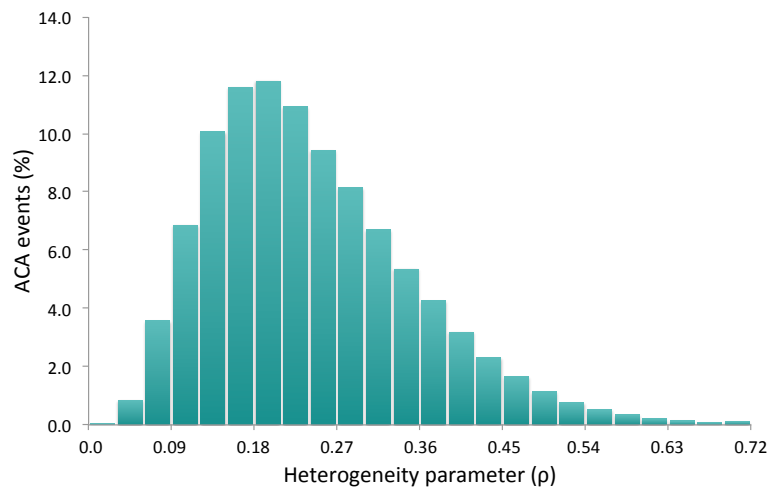


Figure 2. Heterogeneity parameter distribution for ACA events over the South East Atlantic Ocean in June to August 2008.

In the manuscript, page 25553 lines 9 to 11 have been replaced by:

To process the cloud field, the inhomogeneity parameter ρ has been fixed at 0.6, which represents a standard value for stratocumulus clouds [Szczap et al., 2000a & 2000b]. A statistical analysis of

the inhomogeneity parameter has been performed over the ACA scene sampled by the algorithm. It shows that $\rho = 0.6$ can be considered has a high value in this study.

25535

line 2: The last ones -> The latter

line 13: thanks to -> using

These sentences have been corrected.

line 26: "Over a bright surface such as clouds": Clouds are not surfaces, please rephrase.

“Surface” has been replaced by “scene”.

line 28: darkening effect -> darkening

25537

line 4: couple -> number

The manuscript has been modified according to the reviewer suggestion.

line 9: Since -> When I think the consistency shown in Jethva et al (2014) does not yet warrant the claim that this can be done in general.

It is now mentioned that this analysis has been performed for a case study:

Jethva et al. [2014] have carried out a multi-sensor comparison of the above-cloud AOT retrieved from different sensors on board NASA’s A-train satellite for a biomass burning event off the South West African coast.

lines 11-13: "Though, ACAOT retrieval techniques presented above generally require an assumption on the absorption character of the overlying particles or do not enable to estimate it." This sentence is unclear, please rephrase.

This sentence has been rephrased:

However, most of the ACAOT retrievals presented above do not evaluate the aerosol single scattering albedo.

line 18: latest -> latter

The manuscript has been corrected, thank you.

line 21: "it becomes hazardous for coarse mode particles" -> "it cannot be applied to coarse

mode particles."

This sentence has been modified:

While this method is expected to work efficiently for fine mode aerosols as their interactions at longer wavelengths are minimal or even nil, it may not work for coarse mode dust aerosols due to their radiative influence at longer wavelengths.

line 23: scenes -> in the scene

25538

lines 3-4: remove "based on exact modeling"

These modifications have been included to the manuscript.

lines 4-6: "Beyond their types, aerosol absorption properties are expected to vary a lot depending on space, time and formation processes (Dubovik et al., 2002) and thus, resulting on different radiative responses." This sentence is unclear, especially 'beyond their types', please rephrase.

Similarly, the words "Consequently" (line 6) and "Similarly" (line 7) indicate a reasoning in the text that's not there. Please, rephrase using a clear reasoning or simply sum up the paper's contents.

This part of the introduction has been rephrased:

Both algorithms have been applied to three events with contrasted aerosol properties: absorbing biomass burning aerosols off the South West coast of Africa, scattering ones from Siberia and Saharan dust. Then, aerosol and cloud properties as well as the DRE have been evaluated and averaged through August 2006 over the South East Atlantic Ocean.

line 17: thanks to -> owing to

lines 20-21: all along this paper -> in this paper

lines 21: would refer -> refers

25539

line 3: angle -> angles

line 5: are -> is

These corrections have been made, thank you.

line 10: Figure 2 is valid for fine mode particles (0.1 micron), but coarse mode particles are not mentioned here. How do coarse mode particles effect the (polarized) signal? More importantly: What is the uncertainty in the retrieved aerosol parameters? Is it the same for the fine and the coarse mode? And how does this uncertainty effect the uncertainty in the final DRE?

The polarized signature obtained for dust and fine mode aerosols above clouds is displayed in Fig. 3. Contrary to fine mode aerosols, mineral dust particles do not generate an important polarized signal at side scattering angle. However, they strongly attenuate the cloud bow (at scattering angle around 140°). This attenuation is almost spectrally neutral between 670 nm and 865 nm and is directly related to the total AOT for coarse mode aerosols. Let us add that the entire polarized signal is used to retrieve the AOT at 865 nm for dust while only measurements acquired for scattering angle lower than 130° are kept to retrieve the scattering AOT for fine mode aerosols (cf. Fig. 4 in Waquet et al., 2013). The complex part of the refractive index is not expected to vary a lot at 865 nm. Consequently, the same assumption on the SSA at 865 nm is used in the polarized and the total radiance part of the retrieval for dust (i.e. $SSA_{865\text{nm}} = 0.984$). Then, the second part of the retrieval consists in the evaluation of the COT and the dust absorption at 490 nm.

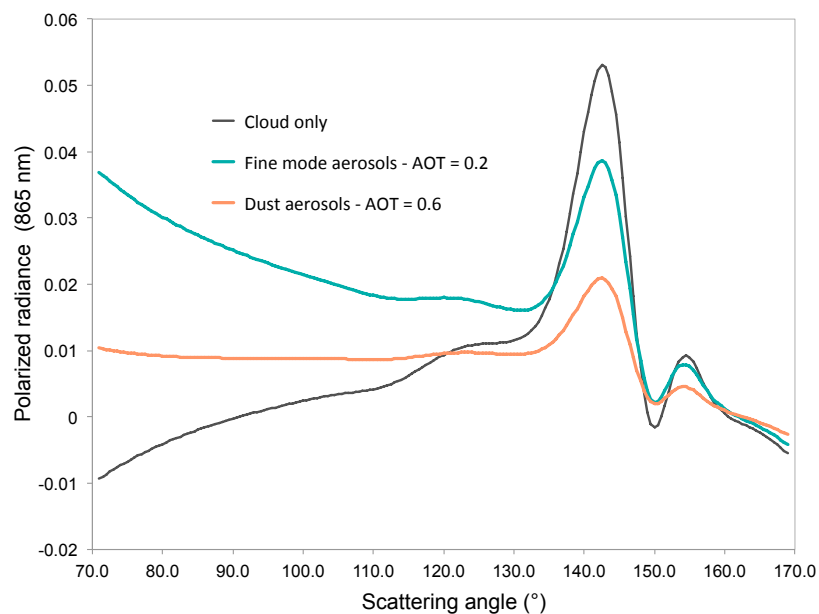


Figure 3. Simulated polarized radiance at 865 nm plotted against the scattering angle. Black line corresponds to the cloud only ($COT = 10$, $r_{\text{eff}} = 10 \mu\text{m}$). Green line corresponds to a fine mode aerosol layer ($r_{\text{eff}} = 0.1 \mu\text{m}$) above cloud with $AOT_{865\text{nm}} = 0.2$. Dust aerosols ($AOT_{865\text{nm}} = 0.6$) above cloud are represented in orange. (Extracted from Waquet et al., 2013.)

Waquet, F., Cornet, C., Deuzé, J. L., Dubovik, O., Ducos, F., Goloub, P., Herman, M., Lapyonok, T., Labonnote, L., C., & Vanbauce, C. (2013). Retrieval of aerosol microphysical and optical properties above liquid clouds from POLDER/PARASOL polarization measurements. *Atmospheric Measurement Techniques*, 6(4), 991-1016.

line 11-12: "In case of clean sky condition (i.e. without aerosols), the total radiances scattered by cloud water droplets are expected to be relatively spectrally independent from the UV to the Short Wave InfraRed (SWIR) part of the spectrum." I think this is not "expected", but shown in other studies, e.g. De Graaf et al (2012), using SCIAMACHY measurements.

This clarification has been added to the manuscript:

In case of clean sky condition (i.e. without aerosols), the total radiances scattered by cloud water droplets are relatively spectrally independent from the UV to the Short Wave InfraRed (SWIR) part of the spectrum [De Graaf et al., 2012].

line 22: .. for a given aerosol size distribution." In fact, this size distribution is not given at all. Please, indicate which experiments were performed. If necessary, add tables with all relevant cloud and aerosol parameters listed, so results can be checked and understood.

This sentence has been rephrased and the caption of Fig. 3 has been completed:

In the same way as Fig. 3 in the study of Jethva et al. [2013], Fig. 3 highlights the color ratio effect. The radiance ratio (L_{490}/L_{865}) is plotted against the SWIR radiance (L_{865}) for several Cloud Optical Thicknesses (COT) and for aerosols with an effective radius of 0.1 μm .

25540

line 11-12: "Meanwhile, the data used in this paper corresponds to the previous version." Please, give version numbers and description, which will be important for readers who know this. Be exact.

The information about the data version is mentioned in the manuscript (i.e. PARASOL Collection 2 v02.04).

lines 20-22: Again, please provide a table with all relevant information.

A precise description of the models used in the LUT is given in the table below (added to the manuscript):

	Polarized LUT	Total radiance LUT
Aerosols models		
Vertical distribution	gaussian layer with a mean altitude of 3 km	homogeneous layer between 2 and 3 km
<u>Fine mode:</u>		
Size distribution	lognormal distribution with $\sigma_f = 0.4$ $r_{\text{eff}} = 0.06$ to $0.16 \mu\text{m}$ (by $0.02 \mu\text{m}$ step)	
Refractive index	1.47 – i.0.01	1.47 – i.k with k = 0.00 to 0.05 (by 0.0025 step)
<u>Dust:</u>		
Size distribution	bimodal lognormal distribution with $\sigma_f = 0.4$ $r_{\text{eff, fine}} = 0.35 \mu\text{m}$ $r_{\text{eff, coarse}} = 2.55 \mu\text{m}$	
Refractive index	1.47 – i.0.0007	1.47 – i.k $k_{865\text{nm}} = 0.0007$ $k_{490\text{nm}} = 0.0$ to 0.004 (by 0.0005 step)
Cloud models		
Vertical distribution	homogeneous layer from 0 to 0.75 km	homogeneous layer from 0 to 1 km
Size distribution	gamma law with $v_{\text{eff}} = 0.06$	
	$r_{\text{eff}} = 5$ to $26 \mu\text{m}$ (by $1 \mu\text{m}$ step)	$r_{\text{eff}} = 10 \mu\text{m}$
Refractive index		$m_{r,490\text{nm}} = 1.338$ $m_{r,670\text{nm}} = 1.331$ $m_{r,865\text{nm}} = 1.330$

Table 1. Aerosol and cloud model properties used to compute the polarized and total radiance LUT of the POLDER algorithm.

25541

line 2: a SD -> a standard deviation (SD)

line 3: thanks to -> using

line 5: one -> AOT

The manuscript has been corrected as suggested by the reviewer.

line 7: "We consider that the aerosol size corresponds to the one of the nearest model". How is the data fitted and what is the critical selection criterion for aerosol model/type? Does this mean only aerosol optical properties interpolated and not the size distribution?

The size distribution is not interpolated. The retrieval of the scattering AOT is attempted at 6 km x 6 km resolution using polarized radiances at 670 and 865 nm. A first estimation of the

total AOT is made based on an assumed complex part of the refractive index. The AOT at both wavelengths is then filtered and aggregated from 6 km x 6 km to 18 km x 18 km. The angström exponent is calculated at the lowest resolution. We consider that aerosols have the size distribution corresponding to the model with the nearest angström exponent. The sentence has been rephrased:

We consider that the aerosol size corresponds to the one of the model with the nearest model (i.e. not interpolated).

lines 14-15: "For the fine mode, k varies from 0.00 to 0.05" Which values have been used? Be specific.

The values used in the LUT are mentioned in the Table 1.

lines 15-16: "...it is assumed to be the same at both wavelengths since a weak variation of this parameter is expected between the used bands.." Why since? Do you mean ONLY a weak variation is expected? Then rephrase it like that.

The sentence has been rephrased:

... it is assumed to be the same at both wavelengths because only a weak variation of this parameter is expected between the used bands ...

line 19: radiations -> radiation

This correction has been made, thank you.

25542

lines 3-4: "The retained solution is the one that minimizes the least square error term." This is the usual approach. But please provide the equation that is actually minimized.

The equation of the error term ε has been added to the manuscript

$$\varepsilon = \sum_{i=1}^{N_{\Theta}} \sum_{j=1}^{N_{\lambda}} [L_{ij}^{meas}(\Theta) - L_{ij}^{calc}(\Theta)]^2 \quad (3)$$

L referring to measured (*meas*) and calculated (*calc*) radiances and Θ being the scattering angle.

line 6: thanks to -> using

line 13: level -> levels

25543 *line 19: of -> off*

These words have been corrected, thank you.

25544

lines 3-6: "To finish with the assumptions about aerosols, we have taken an interest in the altitude of the aerosol layer. We have processed the signal for an aerosol top altitude of 4 and 6km while the aerosol layer reaches 3km in the LUT. However, the results are not displayed since they do not have shown any impact." The purpose of the first sentence is unclear. This is an clear result, and should be mentioned as part of the complete sensitivity study.

The paragraph has been rephrased:

The last assumption about aerosols that has been investigated concerns the vertical distribution of the aerosol layer. We have processed the signal for an aerosol top altitude of 4 and 6 km and the algorithm has retrieved the correct aerosol and cloud properties. In polarization, the bands used to retrieve the scattering AOT (i.e. 670 and 865 nm) are weakly impacted by the molecular contribution. Aerosols in the clouds do not contribute to the polarized signal. Hence the polarized radiances are not impacted by the aerosol vertical distribution as long as the aerosol layer is distinct from the cloud.

line 15: At last -> Lastly

25545

line 6: thanks to -> based on

The manuscript has been modified according to the reviewer suggestion.

line 23: is weakly -> is only weakly

This sentence has been rephrased:

The cloud top height is derived from the POLDER apparent O₂ cloud top pressure [Vanbauce et al., 2003] since the O₂ retrieval allows a reliable estimation of the cloud top height in the presence of an aerosol layer above [Waquet et al., 2009].

25546

Line 1: "The ACA scenes have been selected since they are very usual at global scale." I'm not sure what is intended here. ACA scenes are not very common globally. Change to "Common/representative ACA scenes were selected?"

The sentence has been removed.

lines 11-12: "biomass burning particles are frequently observed around the Southern Africa due to man made vegetation fires" -> biomass burning particles, due to man made vegetation fires,

are frequently observed around the Southern Africa.

line 12 : in the same time -> at the same time

lines 13-14: the deck stratocumulus deck does not favor long-range transport, the wind does, or meteorological conditions. Please, rephrase.

The beginning of the section has been rephrased:

From June to October, biomass burning particles, due to man made vegetation fires, are frequently observed above the persistent deck of stratocumulus covers off the South West African coast.

line 15: an important amount -> a large amount (or better just biomass burning aerosols were detected/observed).

The sentence has been rephrased:

On August 4th 2008 (Fig. 6a), biomass burning aerosols have been observed over clouds.

line 16: The aerosol layer over the Atlantic Ocean is very often a few kilometers thick. If this is the case, please give more information on the height than just one position of 3 km. Was this the average weighted height, does it extend from the cloud top to 3 km? Or further. And how do you treat that in the LUT?

The aerosol layer is located between 3 and 5 km and does not touch the cloud layer located 2 km below. The information about the vertical distribution of the aerosol layer is now given Table 1. As shown in section 2.4, the algorithm is not sensitive to the aerosol altitude.

line 19: The ACAOT value of 0.74 is not shown in the plot! The ACAOT in Fig 6a ranges up to 0.3. After further reading I noticed that the range scales were cut in the plot (or so I assume). This should be corrected in Figs. 6,7, and 8, see the comments on those Figures elsewhere.

25547

line 1: "is respectively of 0.875 and 0.840 at 550 and 865 nm" -> "is 0.875 and 0.840 at 550 and 865 nm, respectively"

line 10: "that takes into the" -> that takes into account the

These sentences have been corrected as suggested by the reviewer.

lines 14-15: "due to the logarithmic relation curve between radiances and with COT". This is bad English, please rephrase.

This sentence has been replaced by:

The impact of the aerosol absorption on the signal gets bigger as the COT increases.

line 16: "the bias is around 15". The highest values shown is 8. Please, correct.

line 18: "As expected for very" -> As expected for highly

This sentence has been modified.

line 19: "DRE up to 195.0". The maximum value shown in 100.

25548

line 2: "due to" -> and / following

The manuscript has been corrected.

lines 5 and 6: "important". Why important? To you? Rather say 'Large'. Or better yet, stay objective.

“Important” has been replaced by “non-negligible”.

line 8: The -> On

The sentence has been corrected.

line 17: peak at 3.0. Not in range of figure

line 19: "the retrieved models" -> the retrieved radii

line 27 "ones" -> ones,

These modifications have been made.

25549

lines 1-3: Can you explain this? Do they have a different origin? Or different pathway/history?

This is most likely explained by the difference of age between the two plumes. Back trajectories suggest that air masses left inland Russia 3 days before arriving to the Southern area while it took only 1 day to arrive in the Northern part of the plume. This explanation has been added to the manuscript.

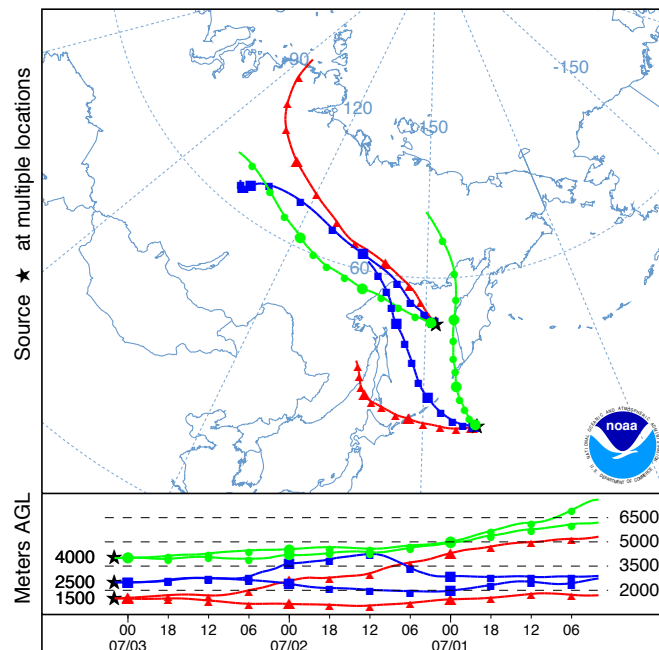


Figure 4. Air mass backward trajectories calculated for altitudes equal to 1.5 km, 2.5 km and 4 km and ending the 3 July 2008 on the area where aerosols above clouds have been detected by POLDER.

line 8: "bias up to +12". Max in Figure is 4. line 9: "bias up to -10.7" Min in Figure is -4 lines 12 and 14: Max and minimum DRE values are not in the Figure.

lines 13-14: "Again, the approximate expression (Eq. 1) can clarify both situations." I think clarification should be a physical explanation, e.g. the one that Eq 1. is based on. Please, rephrase.

The sentence has been rephrased:

As shown in Eq. (1), the sign of the perturbation depends on the balance between the up-scattering and the absorption of the aerosol layer.

lines 15-20: the values are not in the figure

25550

line 8: "southern area" -> "western part", to be consistent in the text.

lines 11-12: "closely look alike" -> are close

line 12: a lot -> strongly

The manuscript has been modified as suggested by the reviewer.

lines 12-14: Add a reference to Haywood et al (2004), who first evaluated this.

The reference has been added, thank you.

line 14: overestimate -> overestimates

line 22: noticed -> notice

25551

lines 17-20: the values given are not in the figure.

25552

line 2: "between the 9 and the 17 August." -> between 9 and 17 August.

lines 7-8: the values are not in the plot.

line 12: observed -> observe.

These corrections have been done.

line 13-15: This point should be stressed more. The data selected for this manuscript are cloud with $COT > 3$ and $CF=1$, which will give a high bias of DRE values. Therefore, the results cannot readily be compared to the results of e.g. De Graaf et al. (2012) who used $CF < 1$ and $COT < 3$.

The end of the paragraph has been rephrased to accentuate this point and the captions of Fig. 10 and 11 have been completed:

However, it has to be noted that these two estimations cannot be directly compared because the SCIAMACHY aerosol DRE has been determined for AAC scenes with a Cloud Fraction (CF) larger than 0.3 while the method developed here is restricted to optically thick clouds ($COT > 3$) with $CF = 1$. Thus, these selection criteria of the AAC scenes lead to a high bias of the DRE. Also, the two satellite instruments do not observe the scene at the same time. Changes of the scene between the two measurements [Min et al., 2014] and the difference of solar zenith angles can explain the remaining discrepancies.

Figure 10. Direct Radiative Effect of aerosols above clouds averaged through August 2006 (a) and number of associated events (b). The DRE has been processed over scenes with a Cloud Fraction (CF) equal to 1 and $COT \geq 3$.

Figure 11. Frequency distribution of the aerosol Direct Radiative Effect above clouds for August 2006 for the South East Atlantic Ocean. Only scenes with $COT \geq 3$ and $CF = 1$ are considered.

25553

line 5 thanks to -> using

line 10 choose -> choosen

line 15: RT -> Radiative Transfer (RT)

line 16: has -> have

The manuscript has been corrected as suggested by the reviewer.

line 27: "11%". Do you mean at 490 nm, and about 14% at 865 nm? Please, be clear and concise.

The sentence has been rephrased:

On average, the plan-parallel cloud (i.e. 1D) produces 9.2% at 490 nm and 12.6% at 865 nm more signal than the heterogeneous cloud field.

25555

line 3: "impact of aerosols." -> impact of aerosols, in case of cloud heterogeneity.

lines 3-4: "The values presented in this paper can be seen as a lower bound for ACA DRE." This is only true for the cloud heterogeneity argument. E.g. the selection criterion of $COT > 3$ will select high values of ACA DRE. Please, rephrase.

The sentence has been rephrased:

For the scenes presented in this paper (i.e. which meet our selection criteria), the obtained values can be seen as a lower bound for the ACA DRE.

Conclusion.

line 20: "The algorithm has shown its ability to accurately retrieved aerosol and cloud properties". This statement is unfortunately untrue, although this would be the desirable conclusion for this manuscript. But the accuracy assessment is missing, so this cannot be concluded.

“Accurately” has been removed of this sentence.

line 23: very -> strongly

25556

line 6: has -> have

line 13: very -> highly

line 19: on -> to

These corrections have been made.

line 23-24: Please, repeat here in the conclusion section that there is a difference between the results of this manuscript and those in the literature, and that those are mainly caused by selection criteria of the clouds.

This part of the conclusion has been rephrased:

The monthly averaged value over the scene is estimated at 33.5 W.m^{-2} , which is of the same order of magnitude as the estimation of De Graaf et al. [2012] (i.e. 23 W.m^{-2}). Let us point out that differences between the result of this study and the literature are expected and are mainly due to the selection of the AAC scenes: this analysis does not include thin clouds (i.e. $\text{COT} < 3$) and scene with fractional cloud coverage which leads to biased high the DRE.

line 24-25: "This analysis shows how important the studies of ACA are for the climate understanding." I don't agree. I think this study shows in three case studies how ACA radiative impacts on clouds can be studied. This will help, climate studies.

This sentence has been removed.

25557

line 10-12: "On the other hand, 3-D effects cause bias on our estimation of the COT. Finally, the homogeneous cloud assumption leads to a slight underestimation of the DRE of aerosols." I think this is an important new conclusion. The effect of homogeneous cloud assumption on the estimation of the DRE should be quantified.

The sentence has been rephrased:

Finally, the homogeneous cloud assumption leads to an underestimation of the DRE of aerosols. This bias remains small in this study because scenes with too heterogeneous clouds are rejected. However, a thorough analysis of the effect of the homogeneous cloud assumption on the estimation of the DRE would provide a significant contribution to the scientific field.

Figure 2: The inset is not explained.

The figure caption has been replaced by:

Figure 2. Simulated polarized radiance at 865 nm plotted against the scattering angle. Black line corresponds to the cloud only ($\text{COT} = 10$, $r_{\text{eff}} = 10 \mu\text{m}$). Colored lines are for an aerosol layer above clouds. The effective radius of aerosols is $0.10 \mu\text{m}$. Several absorption AOT (i.e. various k) have been considered but the scattering AOT is fixed at 0.18. The inset focuses on polarized

radiances of aerosols above clouds for scattering angles between 100° and 130° . Complementary information about vertical distributions and properties of aerosols and clouds can be found in Table 1 (cf. polarized LUT).

Figure 3:

-This figure is very similar to Fig. 3 in Jethva et al (2013). This reference should be added, and in the text the similarity should be noted.

-It is not clear from the text or the figure caption and/or the text in the figure which parameters have been used to generate this plot. In order to understand, compare (e.g. with Jethva et al, 2013) and reproduce the results, it is imperative that all necessary information is available in the paper. Missing are e.g. size distribution, viewing angles, atmospheric parameters, etc.

Lines 21-22 page 25539 have been rephrased:

In the same way as Figure 3 in the study of Jethva et al. [2013], Figure 3 highlights the color ratio effect. The radiance ratio (L_{490}/L_{865}) is plotted against the SWIR radiance (L_{865}) for several Cloud Optical Thicknesses (COT) and for aerosols with an effective radius of $0.1 \mu\text{m}$.

The caption of Figure 3 has been completed:

Figure 3. Radiance ratio $L_{490\text{nm}}/L_{865\text{nm}}$ as a function of the radiance at 865 nm. Signals have been simulated for aerosols with an effective radius of $0.10 \mu\text{m}$, an effective radius of cloud droplet of $10 \mu\text{m}$ (for more information about aerosol and cloud properties and vertical distribution, cf. Table 1, total radiance LUT column). The scattering AOT is set and several absorption AOT as well as several COT are considered. Calculations have been carried out for a solar zenith angle $\theta_s = 41.3^\circ$, a viewing angle $\theta_v = 41.3^\circ$ and a relative azimuth $\phi_r = 180^\circ$.

Figure 4: The annotations are illegible.

Figure 4 has been reconsidered.

1 **Absorption of aerosols above clouds from**
2 **POLDER/PARASOL measurements and estimation of**
3 **their Direct Radiative Effect**

4 **F. Peers¹, F. Waquet¹, C. Cornet¹, P. Dubuisson¹, F. Ducos¹, P.**
5 **Goloub¹, F. Szczap², D. Tanré¹, F. Thieuleux¹**

6 [1]{Laboratoire d'Optique Atmosphérique, Université Lille 1, Villeneuve d'Ascq, France}

7 [2]{Laboratoire de Météorologie Physique, Clermont-Ferrand, France}

8 Correspondence to: F. [Peers \(fanny.peers@ed.univ-lille1.fr\)](mailto:fanny.peers@ed.univ-lille1.fr) and F. Waquet

9 [\(fabien.waquet@univ-lille1.fr\)](mailto:fabien.waquet@univ-lille1.fr)

10 **Abstract**

11 [This study presents an original method to evaluate key parameters for the estimation of the](#)
12 [direct radiative effect of aerosol above clouds: the absorption of the aerosol layer and the](#)
13 [albedo of the underneath cloud](#). It is based on multi-angle total and polarized radiances both
14 provided by the A-train satellite instrument POLDER - Polarization and Directionality of
15 Earth Reflectances. The sensitivities brought by each kind of measurements are used in a
16 complementary way. Polarization mostly translates scattering processes and is thus used to
17 estimate the scattering aerosol optical thickness and the aerosol size. On the other hand, total
18 radiances, together with the scattering properties of aerosols, are used to evaluate the
19 absorption optical thickness of aerosols and the cloud optical thickness. [The retrieval of](#)
20 [aerosol and clouds properties \(i.e. aerosol and cloud optical thickness, aerosol single](#)
21 [scattering albedo and angström exponent\)](#) is restricted to homogeneous and optically thick
22 [clouds \(cloud optical thickness larger than 3\)](#). In addition, a procedure has been developed to
23 process the shortwave direct radiative effect of aerosols above clouds. [Three case studies have](#)
24 [been selected: a case of absorbing biomass burning aerosols above clouds over the South-East](#)
25 [Atlantic Ocean, a Siberian biomass burning event and a layer of Saharan dust above clouds](#)
26 [off the North-West African coast. Besides these](#) case studies (i.e. biomass burning aerosols
27 from Africa and Siberia and Saharan dust), both algorithms have been applied on the South
28 East Atlantic Ocean and results have been averaged through August 2006. The mean direct
29 radiative effect is found to be $33.5 \text{ W}\cdot\text{m}^{-2}$ [\(warming\)](#). Finally, the effect of the heterogeneity

F. Peers 23/2/y 17:33

Supprimé: Peers (fanny.peers@ed.univ-lille1.fr)

F. Peers 23/2/y 17:33

Supprimé: The albedo of clouds and the aerosol absorption are key parameters to evaluate the direct radiative effect of an aerosol layer above clouds. While most of the retrievals of above clouds aerosol characteristics rely on assumptions on the aerosol properties, this study offers a new method to evaluate aerosol and cloud optical properties simultaneously (i.e. aerosol and cloud optical thickness, aerosol single scattering albedo and angström exponent).

F. Peers 23/2/y 17:33

Supprimé: based on exact modeling. Besides the three

F. Peers 23/2/y 17:33

Supprimé: .

1 of clouds has been investigated and reveals that it affects mostly the retrieval of the cloud
2 optical thickness and not much the aerosols properties. The homogenous cloud assumption
3 used in both the properties retrieval and the DRE processing leads to a slight underestimation
4 of the DRE.

5 1. Introduction

6 The quantification of the aerosol radiative impact is one of the largest sources of uncertainty
7 in global climate models [Myhre et al., 2013b]. These uncertainties are mainly related to
8 aerosols in cloudy scenes through direct, semi-direct and indirect effects. The [last two](#)
9 describe the modifications of cloud microphysics because of interactions between clouds and
10 aerosols [Bréon et al., 2002]. Especially, the enhancement of the number of cloud
11 condensation nuclei results in a reduction of cloud droplet size, leading in an enhancement of
12 the cloud albedo [Twomey, 1974 & 1977], a prolongation of their lifetime and a decrease of
13 precipitation [Albrecht, 1989; Ramanathan et al., 2001]. The semi-direct effect refers to
14 changes in cloud formation attributable to the aerosol influences on the vertical stability of the
15 atmosphere [Ackerman et al., 2000; Johnson et al., 2004; Koren et al., 2004; Kaufman et al.,
16 2005]. Finally, the direct effect corresponds to the modification of the amount of solar
17 radiation scattered back to space by the clouds due to the presence of an aerosol layer.
18 [Figure 1](#) illustrates the difference of albedo of a scene $\Delta\rho$ caused by an aerosol layer versus
19 the albedo of the underneath surface. It has been calculated [using](#) the approximate expression
20 given by Lenoble et al. [1982]:

$$\Delta\rho = \rho - \rho_s = \tau(\varpi_0(1 - g)(1 - \rho_s)^2 - 4(1 - \varpi_0)\rho_s) \quad (1)$$

21 ρ_s being the clean-sky albedo of the scene, and ρ , the albedo with aerosols. The aerosol optical
22 thickness τ is related to the amount of particles and corresponds to the sum of the absorption
23 optical thickness τ_{abs} and the scattering one τ_{scatt} . The Single Scattering Albedo (SSA) ϖ_0
24 describes the relative [contribution](#) of the aerosol scattering to the extinction (i.e. scattering
25 and absorption, $\varpi_0 = \tau_{scatt}/\tau$). Finally, the aerosol asymmetry factor g characterizes the
26 preferential direction of the scattered light. The difference of albedo and the shortwave Direct
27 Radiative Effect (DRE) of aerosols are directly proportional. A positive difference of albedo
28 means that the scene appears brighter with aerosols (domination of the scattering process) and
29 thus, it results in a cooling effect (DRE<0). This is the case for aerosols above a dark surface
30 as, for instance, over ocean. Over a bright [scene](#) such as clouds, the sign of the difference of
31 albedo strongly depends on the absorption of the aerosol layer (i.e. the single scattering

F. Peers 23/2/y 17:33

Supprimé: latest ones

F. Peers 23/2/y 17:33

Supprimé:

F. Peers 23/2/y 17:33

Supprimé: thanks to

F. Peers 23/2/y 17:33

Supprimé: importance

F. Peers 23/2/y 17:33

Supprimé: surface

1 | albedo): absorbing aerosols can lead to a darkening (warming effect), but for particles which
2 | would scatter enough, the resulting forcing can be positive (cooling effect). As a consequence,
3 | the improvement of the DRE estimation is driven by the accurate knowledge of the albedo of
4 | the underneath surface, the amount of aerosols and their level of absorption.

5 | In order to constrain numerical models, satellite aerosol retrievals provide essential
6 | information on aerosol and cloud properties, spatial distribution and trends. However, the
7 | study of aerosol layer above clouds is a recent line of research and the radiative effects of
8 | aerosols located above clouds remain unconstrained because most current satellite retrievals
9 | are limited to cloud-free scenes. In addition, the retrieval of cloud properties that determine
10 | the cloud albedo (i.e. the cloud optical thickness and the droplet effective radius) is impacted
11 | by the presence of an aerosol layer above [Haywood et al., 2004; Wilcox et al., 2009;
12 | Coddington et al., 2010] and consequently, it biases the estimation of the DRE. Active
13 | sensors like the Cloud-Aerosol Lidar with Orthogonal Polarization (CALIOP) are dedicated
14 | to the analysis of the atmospheric vertical profile. An operational algorithm [Winker et al.,
15 | 2009 & 2013; Young and Vaughan, 2009] as well as two alternative research methods (i.e.
16 | the de-polarization ratio [Hu et al., 2007] and the color-ratio method [Chand et al., 2008])
17 | enable the retrieval of the Above Clouds Aerosols Optical Thickness (ACAOT).
18 | Nevertheless, passive sensors have also shown an ability to extract information from Above
19 | Clouds Aerosols (ACA) measurements and gain advantage from their wide spatial coverage.
20 | Based on the capacity of aerosols to absorb the UV radiations reflected by the clouds, Torres
21 | et al. [2012] have developed a method to calculate the UV aerosol index and, under some
22 | assumption on the aerosol properties, to retrieve the ACAOT as well as the Aerosol-Corrected
23 | Cloud Optical Thickness (ACCOT) with Ozone Monitoring Instrument (OMI). The amount
24 | of particles above clouds and the ACCOT can also be retrieved simultaneously using
25 | measurements in the visible and in the shortwave infrared from the Moderate Resolution
26 | Imaging Spectroradiometer (MODIS), thanks to the color-ratio method developed by Jethva
27 | et al. [2013].

28 | Contrary to total radiances, polarized measurements are primarily sensitive to the single
29 | scattering process and does no longer depend on the optical thickness of the cloud when it is
30 | thick enough. Waquet et al. [2009 & 2013a] have developed a method to retrieve the ACAOT
31 | at two wavelengths and therefore the angstrom exponent, using polarized radiances from the
32 | Polarization and Directionality of Earth Reflectances (POLDER). Jethva et al. [2014] have
33 | carried out a multi-sensor comparison of the above-cloud AOT retrieved from different

F. Peers 23/2/y 17:33

Supprimé: effect

F. Peers 23/2/y 17:33

Supprimé: a couple of

F. Peers 23/2/y 17:33

Supprimé: an inter-

F. Peers 23/2/y 17:33

Supprimé: exercise on those five retrievals that use

1 sensors [on board NASA's A-train satellite for a biomass burning event off the South West](#)
2 [African coast](#). Considering the different kinds of assumptions and measurements used to
3 retrieve the ACAOT, results have shown good consistency [over the homogeneous cloud](#)
4 [fields](#). Since aerosol and cloud properties are known, it is possible to process the DRE of
5 aerosols above clouds with a radiative transfer model [Chand et al., 2009; Peters et al., 2011;
6 Costantino and Bréon, 2013; Meyer et al., 2013]. [However, most of the ACAOT retrievals](#)
7 [presented above do not evaluate the aerosol single scattering albedo](#). In contrast, the DRE of
8 aerosols above clouds can also be evaluated without making assumptions on aerosol
9 microphysics thanks to the algorithm developed by De Graaf et al. [2012] for Scanning
10 Imaging Absorption Spectrometer for Atmospheric Chartography (SCIAMACHY)
11 measurements. Hyperspectral reflectances from polluted cloud scenes are converted into flux
12 and subtract from the clean cloud one. The [Jatter](#) is modeled thanks to cloud properties
13 derived from SCIAMACHY measurements in the short wave infrared spectrum. [While this](#)
14 [method is expected to work efficiently for fine mode aerosols as their interactions at longer](#)
15 [wavelengths are minimal or even nil, it may not work for coarse mode dust aerosols due to](#)
16 [their radiative influence at longer wavelengths](#).

17 All those retrievals methods have shown that both total and polarized radiances are sensitive
18 to ACA [in the scene](#). The POLDER instrument on PARASOL satellite has the advantage to
19 measure both for several viewing angles and wavelengths, [\[Tanré et al., 2011\]](#). In the next
20 section of this paper, we will evaluate the contribution brought by the combination of the
21 scattering information provided by polarization and the absorption one given by total
22 radiances. We will explore an improved retrieval method for ACA scenes over ocean based
23 on the work of Waquet et al. [2013a] for the three main parameters required to estimate the
24 DRE: the ACAOT, the ACCOT and the SSA of ACA. The previous algorithm has already
25 demonstrated its ability to detect different kinds of particles (i.e. biomass burning, pollution
26 and dust) over clouds at global scale [Waquet et al., 2013b]. In the third section, we will
27 present a module for the processing of ACA DRE. Beyond their types, aerosol absorption
28 properties are expected to vary a lot depending on space, time and formation processes
29 [Dubovik et al., 2002] and thus, resulting on different radiative responses. [Both algorithms](#)
30 [have been applied to three events with contrasted aerosol properties: absorbing biomass](#)
31 [burning aerosols off the South West coast of Africa, scattering ones from Siberia and Saharan](#)
32 [dust](#). Then, aerosol and cloud properties as well as the DRE have been evaluated and
33 averaged through August 2006 over the South East Atlantic Ocean. This region is a key area

F. Peers 23/2/y 17:33

Supprimé: from the

F. Peers 23/2/y 17:33

Supprimé: .

F. Peers 23/2/y 17:33

Supprimé: Though,

F. Peers 23/2/y 17:33

Supprimé: retrieval techniques

F. Peers 23/2/y 17:33

Supprimé: generally require an assumption on the absorption character of the overlying particles or

F. Peers 23/2/y 17:33

Supprimé: enable to estimate it

F. Peers 23/2/y 17:33

Supprimé: latest

F. Peers 23/2/y 17:33

Supprimé: This

F. Peers 23/2/y 17:33

Supprimé: efficient

F. Peers 23/2/y 17:33

Supprimé: long as the aerosol layer does

F. Peers 23/2/y 17:33

Supprimé: affect the infrared signal and thus, it becomes hazardous

F. Peers 23/2/y 17:33

Supprimé: particles

F. Peers 23/2/y 17:33

Supprimé: scenes

F. Peers 23/2/y 17:33

Supprimé: .

F. Peers 23/2/y 17:33

Supprimé: based on exact modeling.

F. Peers 23/2/y 17:33

Supprimé: Consequently, three case studies have been processed. Similarly

1 for the study of aerosol impacts in cloudy skies since biomass burning particles from Africa
2 are usually transported westward over clouds during the dry season. The case studies and the
3 monthly results will be shown in the section 4. Thereafter, the impact of cloud heterogeneity
4 on our estimation of ACA parameters and the DRE will be examined in section 5. Conclusion
5 will be drawn in section 6.

6 2. Retrieval method

7 2.1. Description

8 Polarized measurements can be used to extract information from ACA scenes [Waquet et al.,
9 2009 & 2013a; Hasekamp, 2010; Knobelspiesse et al., 2011] owing to the specific signal
10 produced by cloud liquid droplets. Figure 2 illustrates polarized radiances processed with the
11 SOS code [Deuzé et al., 1989] for a cloudy atmosphere, with (colored lines) and without
12 aerosols above (black line). It should be noted that, in this paper, the radiance refers to the
13 normalized quantity according to the definition given by Herman et al. [2005]. Regarding the
14 clean cloud signal, the amount of polarized light generated by the cloud is very weak at side
15 scattering angles ($70^\circ - 130^\circ$). Also, it does not depend on the COT as long as it is larger than
16 3.0. The aerosol model used for the polluted cloud cases corresponds to fine mode particles
17 with an effective radius of $0.10 \mu\text{m}$. The scattering AOT is fixed (i.e. $\text{AOT}_{\text{scatt}} = 0.18$) while
18 the level of absorption (i.e. AOT_{abs}) has been stretched through the complex part of the
19 refractive index k . The scattering of light by fine mode aerosols causes the creation of an
20 additional polarized signal at side scattering angles. Moreover, in accordance to the sensitivity
21 analysis performed by Waquet et al. [2013a], the effect of absorption processes on
22 polarization is weak for any scattering angles lower than 130° . Thus, the signal is mostly
23 attributable to scattering processes. At the same time, cloud water droplets produce a large
24 peak of polarization at about 140° that is strongly attenuated by aerosols for ACA events.
25 These two effects can be used to derive aerosol scattering properties from multidirectional
26 polarized measurements like the ones provided by POLDER.

27 In case of clean sky condition (i.e. without aerosols), the total radiances scattered by cloud
28 water droplets are relatively spectrally independent from the UV to the Short Wave InfraRed
29 (SWIR) part of the spectrum, [De Graaf et al., 2012]. At the same time, those wavelengths are
30 sensitive to aerosol effects (i.e. absorption and scattering) whose spectral behaviors depend
31 strongly on the microphysics of the particles (e.g. size, chemical composition, shape).

F. Peers 23/2/y 17:33

Supprimé: thanks

F. Peers 23/2/y 17:33

Supprimé: all along the

F. Peers 23/2/y 17:33

Supprimé: would refer

F. Peers 23/2/y 17:33

Supprimé: angle

F. Peers 23/2/y 17:33

Supprimé: are

F. Peers 23/2/y 17:33

Supprimé: expected to be

F. Peers 23/2/y 17:33

Supprimé: .

1 Consequently, the presence of an aerosol layer above clouds affects the signal that can be
2 measured by satellite instruments: the spectral tendency of aerosol absorption leads to a
3 modification of the apparent color of the clouds. Simulations of the upwelling radiance at 490
4 and 865 nm for ACA events have been processed with a radiative transfer code based on the
5 adding-doubling method [De Haan et al., 1987]. In the same way as Fig. 3 in the study of
6 Jethva et al. [2013], Fig. 3 highlights the color ratio effect. The radiance ratio (L_{490}/L_{865}) is
7 plotted against the SWIR radiance (L_{865}) for several Cloud Optical Thicknesses (COT) and for
8 aerosols with an effective radius of 0.1 μm . Similarly to the previous figure, the scattering
9 AOT is fixed and several absorption AOT is considered. The complex part of the refractive
10 index k is set equal at both wavelengths. This plot clearly illustrates the enhancement of the
11 spectral contrast with absorption. For a given value of the radiance ratio, the 865 nm band
12 provides the sensitivity to the COT. That is to say, radiances at 490 and 865 nm can be
13 interpreted as a coupled ACCOT and absorption ACAOT as long as the scattering optical
14 thickness of aerosol and their size are known.

15 2.2. POLDER data

16 The POLDER instrument is the main part of the PARASOL's payload (Polarization and
17 Anisotropy of Reflectances for Atmospheric Science coupled with Observations from a Lidar)
18 that have flown from 2004 to 2013, including 5 years as a part of the A-train constellation. It
19 provides radiances for 9 spectral bands between 443 and 1020 nm as well as polarization
20 measurements over 3 (i.e. 490, 670 and 865 nm). Thanks to its 2-dimensional CCD camera,
21 the instrument acquires a series of images, which allow the target to be seen from up to 16
22 viewing angles. The ground spatial resolution of POLDER at nadir is 5.3x6.2 km². A new
23 version of Level 1 (v03.02) products will be released by the CNES by the end of 2014
24 including an improvement of the radiometric calibration [Fougnie et al., 2007]. Meanwhile,
25 the data used in this paper corresponds to the previous version, (i.e. PARASOL Collection 2
26 v02.04).

27 2.3. Algorithm

28 The distinctive feature of the method presented here is to combine the information provided
29 by both total and polarized multidirectional radiances from POLDER. The first step consists
30 in estimating the scattering optical thickness and the aerosol size with polarization. We
31 proceed with the Look Up Table (LUT) approach described by Waquet et al. [2013a].

F. Peers 23/2/y 17:33

Supprimé: Figure 3 displays

F. Peers 23/2/y 17:33

Supprimé: versus

F. Peers 23/2/y 17:33

Supprimé: a given aerosol size distribution

F. Peers 23/2/y 17:33

Supprimé: .

1 Polarized radiances at 670 and 865 nm have been computed with the SOS code [Deuzé et al.,
 2 1989] for seven models of aerosols that follow a lognormal size distribution (cf. Table 1). Six
 3 of them correspond to spherical aerosols from the fine mode with radius from 0.06 to 0.16 μm
 4 and assuming a complex refractive index of $1.47 - 0.01i$. The last one is a nonspherical model
 5 for dust with a refractive index of $1.47 - 0.0007i$. The retrieval of the scattering AOT is
 6 attempted for each $6\text{km} \times 6\text{km}$ POLDER's pixel when the COT given by MODIS is larger
 7 than 3.0. If fine mode aerosols have been identified, the estimation of the scattering AOT is
 8 based on the signal measured for scattering angle lower than 130° . At that point, a first
 9 estimation of the extinction AOT is made based on the absorption assumed for the selected
 10 aerosol model (i.e. $k_{\text{assumption}}$). Results are then subjected to several filters in order to improve
 11 their quality: data must be well fitted, clouds have to be homogeneous and both cloud edges
 12 and cirrus are rejected according to criteria based on POLDER and MODIS products. Filtered
 13 AOT are then aggregated from $6\text{ km} \times 6\text{ km}$ to $18\text{ km} \times 18\text{ km}$ and pixels with a Standard
 14 Deviation (SD) of the AOT larger than 0.1 are excluded in order to prevent cloud edge
 15 contamination. Eventually, the scattering AOT is recovered using the SSA of the aerosol
 16 model with the same absorption assumption used at first (i.e. $k_{\text{assumption}}$):

$$\tau_{\text{scatt},\lambda} = \varpi_{0,\lambda,k_{\text{assumption}}} \tau_{\text{ext},\lambda,k_{\text{assumption}}} \quad (2)$$

17 τ_{scatt} being the scattering AOT, τ_{ext} the extinction AOT retrieved with polarization, ϖ_0 the SSA
 18 corresponding to the model used for the retrieval and λ referring to the wavelength. We
 19 consider that the aerosol size corresponds to the one of the model with the nearest model (i.e.
 20 not interpolated).

21 The second part of the method aims at evaluating the absorption of ACA and the ACCOT
 22 using multidirectional radiances at 490 and 865 nm and the information on properties already
 23 provided by polarization. Once again, the process consists in a comparison with radiance
 24 LUT. For computing time reason, we have chosen to process radiances with the adding-
 25 doubling code [De Haan et al., 1987] instead of the one used for the polarized LUT (i.e. SOS
 26 code). The models are based on the 7 ones previously considered with several imaginary parts
 27 of the refractive index k (cf. Table 1). For the fine mode, k varies from 0.00 to 0.05 and it is
 28 assumed to be the same at both wavelengths because only a weak variation of this parameter
 29 is expected between the used bands for this type of aerosols. On the opposite, the dust
 30 complex part of the refractive index should have a pronounced spectral dependence because
 31 of the presence of iron oxide that absorbs blue and UV radiation. Consequently, we have set
 32 the value of k to 0.0007 at 865 nm, based on the result obtained with the research algorithm

F. Peers 23/2/y 17:33

Supprimé: .

F. Peers 23/2/y 17:33

Supprimé: Given the absorption defined for these models, the algorithm evaluates the extinction AOT.

F. Peers 23/2/y 17:33

Supprimé: $6 \times 6 \text{ km}^2$

F. Peers 23/2/y 17:33

Supprimé: $6 \times 6 \text{ km}^2$

F. Peers 23/2/y 17:33

Supprimé: $18 \times 18 \text{ km}^2$

F. Peers 23/2/y 17:33

Supprimé: standard deviation

F. Peers 23/2/y 17:33

Supprimé: calculated thanks to the SSA:

F. Peers 23/2/y 17:33

Supprimé: one

F. Peers 23/2/y 17:33

Supprimé: .

F. Peers 23/2/y 17:33

Supprimé: .

F. Peers 23/2/y 17:33

Supprimé: since

F. Peers 23/2/y 17:33

Supprimé: radiations

1 developed in Waquet et al. [2013a]. The absorption at 490 nm is evaluated in a range of k
 2 | from 0.000 to 0.004. Considering cloud properties (cf. Table 1), the droplet effective size
 3 distribution is considered to follow a gamma law with an effective variance of 0.06. The
 4 cloud droplet effective radius is set to 10.0 μm since the wavelengths selected for the retrieval
 5 | do not have a noticeable sensitivity to this parameter [Rossow et al., 1989]. The cloud top
 6 height is fixed at 1 km and the aerosol layer is located between 2 and 3 km. Finally, the
 7 reflection of the solar radiation by the ocean surface (i.e. the sunglint), which can be
 8 significant for optically thin clouds, is taken into account by considering surface wind speed
 9 from 2.0 to 15.0 m.s^{-1} [Cox and Munk, 1954]. The input data are the multidirectional
 10 radiances at 490 and 865 nm from $6 \times 6 \text{ km}^2$ from POLDER, the scattering ACAOT and the
 11 aerosol model previously determined and the surface wind speed from modeling. The retained
 12 | solution is the one that minimizes the least square error term ε :

$$\varepsilon = \sum_{i=1}^{N_a} \sum_{j=1}^{N_s} [L_{ij}^{meas}(\Theta) - L_{ij}^{calc}(\Theta)]^2 \quad (3)$$

13 | L referring to measured (*meas*) and calculated (*calc*) radiances and Θ being the scattering
 14 angle. In accordance with the operational product of POLDER clear-sky retrieval, the
 15 angström exponent α is calculated from the optical thicknesses τ at 670 and 865 nm using the
 16 expression below:

$$\alpha = - \frac{\log(\tau_{670 \text{ nm}} / \tau_{865 \text{ nm}})}{\log(670.0 / 865.0)} \quad (4)$$

17 An example of total radiances measured at 490 and 865 nm by POLDER for one pixel is
 18 | given in Fig. 4a and 4b respectively. The estimation of the cloud and aerosol properties has
 19 been derived thanks to the method described hereinbefore. Aerosols belong to the fine mode
 20 with an ACAOT of 0.142 at 865 nm and a complex part of the refractive index k at 0.035. The
 21 COT is evaluated at 12.4. Figure 4 also illustrates the signal modeled during the retrieval for
 22 | different levels of absorption with an ACCOT corresponding to our solution. For completely
 23 scattering particles (i.e. $k = 0.00$), one can note that SWIR and visible radiances reach
 24 approximately the same levels. In that case, the scene appears almost spectrally neutral. When
 25 the absorption AOT is increased (i.e. increasing of the complex part of the refractive index k),
 26 both radiances decrease. However, one can notice the increasing gap between visible and
 27 SWIR radiances as the absorption grows, called the color ratio effect. Since aerosol absorption

F. Peers 23/2/y 17:33
Supprimé: .

F. Peers 23/2/y 17:33
Supprimé: .

F. Peers 23/2/y 17:33
Supprimé: .

F. Peers 23/2/y 17:33
Supprimé: thanks to

F. Peers 23/2/y 17:33
Supprimé: Figure

F. Peers 23/2/y 17:33
Supprimé: level

F. Peers 23/2/y 17:33
Supprimé: UV

F. Peers 23/2/y 17:33
Supprimé: level

F. Peers 23/2/y 17:33
Supprimé: it is interesting to

F. Peers 23/2/y 17:33
Supprimé: that

F. Peers 23/2/y 17:33
Supprimé: UV

F. Peers 23/2/y 17:33
Supprimé: increases

F. Peers 23/2/y 17:33
Supprimé: .

1 [has a spectral signature, it produces stronger absorption effects at shorter wavelengths than at](#)
2 [longer ones.](#)

3 2.4. Sensitivity analysis

4 The method developed hereinbefore requires assumptions at different stages of the retrieval.
5 The aim of this section is to analyze the resulting impact on the retrieval. To serve this
6 purpose, POLDER's observations have been modeled with the same radiative transfer code
7 used for the LUT, considering several aerosol and cloud models. Errors due to the
8 polarization part of the retrieval are investigated and then, impacted on the total radiances
9 step.

10 [We first examine the assumption regarding aerosol properties. In order to retrieve the](#)
11 [scattering AOT, it is assumed that polarized measurements are weakly sensitive to aerosol](#)
12 [absorption. This approximation is expected to become less consistent when the aerosol layer](#)
13 [is very absorbing \(i.e. large AOT and low SSA\). This leads to an error in the estimation of the](#)
14 [scattering AOT that could affect the retrieval of the SSA. The second assumption concerns](#)
15 [the real part of the refractive index \$m\$ fixed at 1.47 for the retrieval. To assess the impact of](#)
16 [these assumptions, we have considered 3 absorbing aerosol models with different refractive](#)
17 [indices \$n\$: 1.42 - 0.03i, 1.47 - 0.03i and 1.52 - 0.03i corresponding to a SSA at 865 nm of](#)
18 [0.735, 0.772 and 0.801, respectively. The real parts of the refractive indices have been chosen](#)
19 [to be representative of the variability observed within the aerosol fine mode \[Dubovik et al.,](#)
20 [2002\]. Aerosols have an effective radius of 0.1 \$\mu\text{m}\$ and their mean altitude is 3 km. The cloud](#)
21 [layer used to model the signal has a top altitude at 0.75 km, an optical thickness of 10 and a](#)
22 [droplet effective radius of 10 \$\mu\text{m}\$. Total and polarized radiances have been simulated for](#)
23 [absorbing aerosol layers with increasing AOT. Finally, the DRE of aerosols has been](#)
24 [processed using the radiative transfer code GAME \[Dubuisson et al, 2004\], based on the](#)
25 [properties of the modeled scene on the one hand, and those retrieved by the algorithm on the](#)
26 [other hand. In Fig. 5, the aerosol and cloud parameters retrieved \(green lines\) and used in the](#)
27 [input simulations \(grey lines\) are plotted as a function of the AOT at 865 nm. The middle](#)
28 [column \(i.e. \$n = 1.47 - 0.03i\$ \) shows the biases due to the approximation that polarized](#)
29 [radiances translate the scattering process only while the left and the right ones \(i.e. \$n = 1.42 -\$](#)
30 [0.03i and 1.52 - 0.03i\) present also the effect due to the assumption on the real part of the](#)
31 [refractive index.](#)

F. Peers 23/2/y 17:33

Supprimé: making

F. Peers 23/2/y 17:33

Supprimé: The input parameters corresponding to the referring state are $AOT_{865nm} = 0.20$, $AOT_{scat,865nm} = 0.18$, $r_{eff,aer} = 0.10 \mu\text{m}$, $n = m - ik = 1.47 - 0.001i$ for the aerosol properties and $COT_{550nm} = 10$, $r_{eff,cloud} = 10 \mu\text{m}$ and $z_{top,cloud} = 1 \text{ km}$ for the cloud properties.

F. Peers 23/2/y 17:33

Supprimé: The results of this sensitivity study are summarized in Table 1 to 3.

F. Peers 23/2/y 17:33

Supprimé: We first examine the assumption regarding the weak sensitivity of polarized measurement to absorption process. The complex refractive index k for the fine mode LUT has been fixed at 0.01 for polarized radiances. We have modeled total and polarized signals for $k = 0.005$ and 0.02, a scattering ACAOT of 0.18 and a COT of 10.0. The second assumption concerns the real part of the refractive index fixed at 1.47 for the retrieval. The impact of this assumption was analyzed by considering aerosols with a real part of the refractive index of 1.41 and 1.53. The results of the retrieval are reported in Table 1. The evaluation of fine mode aerosol properties seems to be weakly impacted by the approximations on the particle refractive index. The most unfavorable case concerns aerosols with a low real part of the refractive index (e.g. industrial aerosols) because it might cause an underestimation of both the AOT (-27 %) and the aerosol size (-0.02 μm). On the other hand, one can notice that the error on the total AOT is partly counterbalance by an overestimation of the complex part of the refractive index. Thus, the resulting bias for the absorption optical thickness falls of to -6 %. Also, let us point out the low error due to the assumption on aerosol absorption during the polarized part of the retrieval. Of course, we expect larger biases for larger AOT. However, the quantity of aerosols chosen to process the synthetic radiances is representative of the ACA events that have been already observed in Waquet et al. [2013b]. - ... [1]

1 - The first two rows display the total and the scattering AOT. For $m = 1.42$ and 1.47 ,
2 the algorithm underestimates the AOT. This error comes from the underestimation of the
3 scattering AOT during the polarized part of the retrieval. For AOT lower than 0.2 , we observe
4 a bias around 20% on the AOT. In case of extreme events, with AOT around 0.6 (i.e. 1.5 at
5 550 nm), the AOT is underestimated of 26.7% for $m = 1.47$ and 24.1% for $m = 1.42$,
6 respectively. On the opposite, the algorithm overestimate the AOT when $m = 1.52$. It has to
7 be noted that the retrieved aerosol radius is larger than the one use to model the signal
8 ($0.12 \mu\text{m}$ instead of $0.1 \mu\text{m}$). In that case, the largest error on the AOT (i.e. 25.3%) is
9 observed at $\text{AOT} = 0.2$. Then, the error slowly decreases with the AOT because of the
10 compensation with the aerosol absorption, reaching 16.8% at $\text{AOT} = 0.6$.

11 - Rows 3 and 4 of Fig. 5 show the absorption AOT and the SSA versus the total AOT.
12 In spite of the error on the scattering AOT, it is interesting to observe that the biases on the
13 absorption AOT are small. Because of the sensitivity of total radiances to the absorption of
14 the aerosol layer, the algorithm compensates the bias on the scattering AOT due to the first
15 part by an error on the SSA. As a consequence, a negative error (resp. positive) in the
16 scattering AOT goes together with an underestimation (resp. overestimation) of the SSA. For
17 $\text{AOT} = 0.6$, a bias of -0.055 has been observed for $m = 1.42$ and 1.47 and $+0.033$ for
18 $m = 1.52$, respectively.

19 - Plots of the 4th row represent the retrieved COT. They reveal that both the
20 approximation regarding polarized radiance and the assumption on the real part of the
21 refractive index have a limited impact on the COT estimation. In this analysis, the largest bias
22 is ± 0.3 on the COT.

23 - Finally, the last line focuses on the evolution of the DRE of aerosols with the
24 modeled AOT. The DRE estimated with aerosol and cloud properties retrieved by the
25 algorithm is close to the one processed with the properties of the modeled scene. This can be
26 explained by the reliable estimation of the aerosol layer absorption: as suggested by Eq. (1),
27 the absorption AOT is the leading parameter in the estimation of the DRE for large values of
28 the albedo of the underneath scene. The largest bias ($+9.7 \text{ W.m}^{-2}$) has been obtained for
29 $\text{AOT} = 0.6$ and $m = 1.52$. Otherwise, the bias is always lower than $\pm 6.4 \text{ W.m}^{-2}$ for AOT lower
30 than 0.2 and lower than $\pm 1 \text{ W.m}^{-2}$ for AOT lower than 0.1 .

31 In a second place, we look at the assumption on the size distribution of the coarse mode
32 particles. For the retrieval, we only consider one model for dust. It is defined by a bimodal
33 lognormal size distribution with an angström exponent of 0.36 [Waquet et al., 2013a]. The

F. Peers 23/2/y 17:33

Supprimé: This parameter

1 | signal has been modeled for coarse mode particles with an angström exponent of 0.02 and 0.6
 2 | and an AOT = 0.6. The method appears to allow a consistent evaluation of the SSA at 490 nm
 3 | (error < 1%) in spite of the error on the optical thickness and on the angström exponent (error
 4 | on AOT around 24% and on angström exponent 100%).

5 | The last assumption about aerosols that has been investigated concerns the vertical
 6 | distribution of the aerosol layer. We have processed the signal for an aerosol top altitude of 4
 7 | and 6 km and the algorithm has retrieved the correct aerosol and cloud properties. In
 8 | polarization, the bands used to retrieve the scattering AOT (i.e. 670 and 865 nm) are weakly
 9 | impacted by the molecular contribution. Aerosols in the clouds do not contribute to the
 10 | creation of polarized signal at side scattering angle. Hence the polarized radiances are not
 11 | impacted by the aerosol vertical distribution as long as the aerosol layer is distinct from the
 12 | cloud.

13 | Regarding the cloud hypothesis, we test the impact of considering only one cloud droplet
 14 | effective radius ($r_{\text{eff,cl d}} = 10 \mu\text{m}$) for the estimation of the aerosol absorption and the ACCOT
 15 | by modeling the signal for $r_{\text{eff,cl d}} = 6$ and $20 \mu\text{m}$ with a COT = 10. The approximation
 16 | regarding the effective radius of cloud droplet is the main source of error on the COT
 17 | estimation. While the error on the COT due to aerosol hypothesis does not exceed 3%, this
 18 | one may lead to a bias of $\pm 10\%$ for the COT, which is in agreement with the study of Rossow
 19 | et al. [1989]. However, statistical analysis of the scenes studied hereafter have shown that
 20 | more than 70% of the clouds have an effective radius ranging between 8 and $16 \mu\text{m}$. Lastly,
 21 | we have investigated the influence of the cloud top altitude by considering $z_{\text{top,cl d}} = 2$ and
 22 | 4 km. For each case, the algorithm has retrieved the correct parameters for clouds and
 23 | aerosols.

24 | 3. Radiative Effect Estimation

25 | As previously shown, the accurate knowledge of the aerosol and cloud properties is required
 26 | for estimating the direct radiative forcing due to an aerosol layer above clouds. At the Top Of
 27 | the Atmosphere (TOA), this instantaneous Direct Radiative Effect (DRE) $\Delta F(\theta_s)$ is expressed
 28 | as a flux difference given by:

$$\begin{aligned} \Delta F(\theta_s) &= \left(F^\downarrow(\theta_s) - F_{\text{cloud+aer}}^\uparrow(\theta_s) \right) - \left(F^\downarrow(\theta_s) - F_{\text{cloud}}^\uparrow(\theta_s) \right) \\ &= F_{\text{cloud}}^\uparrow(\theta_s) - F_{\text{cloud+aer}}^\uparrow(\theta_s) \end{aligned} \quad (5)$$

- F. Peers 23/2/y 17:33
Supprimé: perturbed by the consideration of several fraction of the
- F. Peers 23/2/y 17:33
Supprimé: (Table 2).
- F. Peers 23/2/y 17:33
Supprimé: good
- F. Peers 23/2/y 17:33
Supprimé: To finish with the assumptions
- F. Peers 23/2/y 17:33
Supprimé: , we have taken an interest in the altitude
- F. Peers 23/2/y 17:33
Supprimé: while
- F. Peers 23/2/y 17:33
Supprimé: layer reaches 3 km in
- F. Peers 23/2/y 17:33
Supprimé: LUT. However,
- F. Peers 23/2/y 17:33
Supprimé: results
- F. Peers 23/2/y 17:33
Supprimé: not displayed since they
- F. Peers 23/2/y 17:33
Supprimé: have shown any impact.
- F. Peers 23/2/y 17:33
Supprimé: (Table 3),
- F. Peers 23/2/y 17:33
Supprimé: μm
- F. Peers 23/2/y 17:33
Supprimé: μm . The results are given in Table 3.
- F. Peers 23/2/y 17:33
Supprimé: other
- F. Peers 23/2/y 17:33
Supprimé: 2 %, the latest
- F. Peers 23/2/y 17:33
Supprimé:
- F. Peers 23/2/y 17:33
Supprimé:
- F. Peers 23/2/y 17:33
Supprimé: consistent
- F. Peers 23/2/y 17:33
Supprimé:
- F. Peers 23/2/y 17:33
Supprimé: μm . At last
- F. Peers 23/2/y 17:33
Supprimé:
- F. Peers 23/2/y 17:33
Supprimé:

1 θ_s being the solar zenith angle, F^\downarrow the downward flux at the TOA, $F^\uparrow_{cloud+aer}$ the upward flux
2 when aerosols are present and F^\uparrow_{cloud} corresponds to the flux reflected by clouds with no
3 aerosol above.

4 Since the approximate method described earlier (Eq. (1)) could lead to results not correct
5 enough for coarse mode particles, we have chosen to found our approach on exact calculation
6 based on the radiative transfer code GAME [Dubuisson et al, 2004]. Instantaneous shortwave
7 radiative forcing (i.e. from 0.2 to 4 μm) has been precomputed for several solar zenith angles.
8 Regarding fine mode aerosols, they are assumed to be only composed of black carbon. In
9 other words, the imaginary part of the refractive index is constant in the shortwave (grey
10 aerosols) and corresponds to the one retrieved by our algorithm. For dust aerosols, the
11 spectral dependence of the absorption is based on the work of Balkanski et al. [2007],
12 adjusting the UV imaginary part of the refractive index with the retrieved value at 490 nm. In
13 addition to the aerosol and cloud properties derived using the methods described hereinbefore
14 (i.e. ACCOT, ACAOT, the aerosol size and their absorption), the LUT takes into account
15 several cloud droplet effective radii and atmospheric vertical distributions. Those latest are
16 characterized by the cloud top height (considering an aerosol layer between 1 and 2 km above
17 the cloud), the amount of absorbing gases (i.e. ozone and water vapor) and the atmospheric
18 model (i.e. the pressure, temperature and gases vertical profiles). The DRE is obtained by
19 interpolation of the LUT.

20 Regarding the additional input data, the information about the cloud droplets size comes from
21 MODIS [Nakajima and King, 1990]. The cloud top height is derived from the POLDER
22 apparent O2 cloud top pressure [Vanbaue et al., 2003] since the O2 retrieval allows a reliable
23 estimation of the cloud top height in the presence of an aerosol layer above [Waquet et al.,
24 2009]. The ozone and water vapor contents are given by meteorological modeling. Finally,
25 the atmospheric vertical profile depends on the seasons and the geographic location [Cole et
26 al., 1965] (i.e. mid-latitude, tropical, sub-arctic summer and winter).

27 4. Results

28 4.1. Case studies

29 The RGB images of the 3 selected case studies are shown in Fig. 6. The first one (Fig. 6a) is
30 related to a biomass burning event during the dry season in the South of Africa, the second
31 (Fig. 6b) concerns Siberian biomass burning aerosols transported above clouds, and the last

F. Peers 23/2/y 17:33
Supprimé:)
F. Peers 23/2/y 17:33
Supprimé: base
F. Peers 23/2/y 17:33
Supprimé: thanks to
F. Peers 23/2/y 17:33
Supprimé: the aerosol models
F. Peers 23/2/y 17:33
Supprimé: for fine mode

F. Peers 23/2/y 17:33
Supprimé: this method is weakly impacted by
F. Peers 23/2/y 17:33
Supprimé: clouds

F. Peers 23/2/y 17:33
Supprimé: The ACA scenes have been selected since they are very usual at global scale.
F. Peers 23/2/y 17:33
Supprimé: Figure 5
F. Peers 23/2/y 17:33
Supprimé: 5a
F. Peers 23/2/y 17:33
Supprimé: 5b

1 | one (Fig. 6c) is about Saharan dust. For each case, the retrieved parameters (i.e. the ACAOT,
2 | the aerosol scattering albedo, their angström exponent and the ACCOT) will be shown as well
3 | as the estimation of the DRE.

4 | 4.1.1. African biomass burning aerosols

5 | From June to October, biomass burning particles from man made vegetation fires, are
6 | frequently observed above the persistent deck of stratocumulus covers off the South West
7 | African coast. On 4th August, 2008 (Fig. 6a), biomass burning aerosols have been observed
8 | over clouds. Under the CALIOP track (not shown), the aerosol layer is located between 3 and
9 | 5 km and the cloud top at 1 km.

10 | The evaluation of aerosol and cloud properties has been performed over ocean and results are
11 | displayed in Fig. 7. The ACAOT (Fig. 7a) reach high values up to 0.74 at 865 nm. As
12 | expected, aerosols are found to belong to the fine mode with effective radius, from 0.10 μm
13 | close to the coast, to 0.16 μm as the plume shifts to the open sea. The angström exponent
14 | (Fig. 7b), which depends not only on the aerosol size but also slightly on the refractive index,
15 | is around 1.94. Figure 7c shows the low values obtained for the SSA expressing the strong
16 | absorbing capability of these aerosols. The lowest SSAs are about 0.73 at 865 nm near the
17 | coast. These aerosols are associated with a complex part of the refractive index around 0.042.
18 | The average SSA of the scene is of 0.875 and 0.840 at 550 and 865 nm, respectively, which is
19 | consistent with previous African savannah biomass burning retrieval from AERONET
20 | [Dubovik et al., 2002; Sayer et al. 2014] and remote and in-situ measurements from the
21 | SAFARI 2000 campaign [Leahy et al., 2007; Johnson et al., 2008].

22 | The retrieved ACCOT as well as the difference with MODIS observations are shown in
23 | Fig. 7d and 7e. The pattern followed by the ACCOT is close to the one given by MODIS.
24 | However, the comparison between the two methods reveals systematic biases when absorbing
25 | aerosols are above clouds. According to previous studies [Haywood et al., 2004; Wilcox et
26 | al., 2009; Coddington et al., 2010; Meyer et al., 2013; Jethva et al., 2013], the estimation of
27 | the COT that takes into account the aerosol absorption gives higher values than the MODIS
28 | MYD06 cloud product. Because aerosols absorb at the wavelengths traditionally use to
29 | retrieve the COT, the cloud appears darker leading to an underestimation of its optical
30 | thickness. The impact of the aerosol absorption on the signal gets bigger as the COT
31 | increases. Where the clouds are the thickest and the absorption ACAOT the largest (i.e. a

F. Peers 23/2/y 17:33

Supprimé: 5c

F. Peers 23/2/y 17:33

Supprimé: are frequently observed around the Southern Africa due to

F. Peers 23/2/y 17:33

Supprimé: . In the same time, a

F. Peers 23/2/y 17:33

Supprimé: , favoring the long-range transport over the Atlantic Ocean of aerosols above clouds.

F. Peers 23/2/y 17:33

Supprimé: , 4th

F. Peers 23/2/y 17:33

Supprimé: 5a), an important amount of

F. Peers 23/2/y 17:33

Supprimé: has

F. Peers 23/2/y 17:33

Supprimé: detected

F. Peers 23/2/y 17:33

Supprimé: at around

F. Peers 23/2/y 17:33

Supprimé: Figure 6

F. Peers 23/2/y 17:33

Supprimé: 6a

F. Peers 23/2/y 17:33

Supprimé: 6b

F. Peers 23/2/y 17:33

Supprimé: 6c

F. Peers 23/2/y 17:33

Supprimé: respectively

F. Peers 23/2/y 17:33

Supprimé: Figure 6d

F. Peers 23/2/y 17:33

Supprimé: 6e

F. Peers 23/2/y 17:33

Supprimé: bias increases with

F. Peers 23/2/y 17:33

Supprimé: and

F. Peers 23/2/y 17:33

Supprimé: due to the logarithmic relation curve between radiances and with COT

1 small area around (10°S, 8°E)), the bias is around 15. On average over the whole scene,
2 ACCOT is larger than the MODIS value by 1.2.

3 Finally, the DRE has been estimated and is reported in [Fig. 7f](#). As expected for [highly](#)
4 absorbing aerosols, the warming effect reaches high level with DRE up to 195.0 W.m⁻². As
5 suggested by the approximation given by Lenoble et al. [1982] (Eq. (1)), such large values are
6 obtained for an important amount of absorbing aerosols collocated with a very bright cloud
7 (i.e. high COT value). However, 77% of the pixels have a DRE lower than 60 W.m⁻². In
8 contrast, the radiative impact is found to be very weak, even slightly negative, on the south of
9 the scene, where the clouds are the thinnest and the aerosols less absorbing and in small
10 amount. On average over the region, the instantaneous radiative forcing is evaluated at
11 36.5 W.m⁻².

12 4.1.2. Siberian biomass burning aerosols

13 High northern latitudes are also subject to forest fires from June to October. They are mostly
14 from natural origin [following](#) favorable climatic conditions [Stocks et al., 2001] and Siberia is
15 one of the most affected areas by boreal fires [Zhang et al., 2003] leading to [significant](#)
16 production of smoke. These aerosols can be transported over long distance [Jaffe et al., 2004]
17 and may result in [a non-negligible](#) radiative impact [Lee et al., 2005; Péré et al., 2014]. Wild
18 fires have occurred on the Eastern part of Siberia in July 2008 [Paris et al., 2009]. [On 3rd](#) July,
19 aerosols have been detected above clouds (Fig. [6b](#)), over the Sea of Okhotsk. Backward
20 trajectories have shown that they came from the inland of Russia and the MODIS fire product
21 [Giglio et al., 2003] suggests that they may be attributable to fires that took place on the
22 Russian east coast. According to CALIOP, the cloud top is at around 1 km and the aerosol
23 layer is located at about 2 km in the north of the scene (latitude 55°) and goes up to 4 km as
24 we move southward (latitude 45°).

25 The results of the algorithm are reported in [Fig. 8](#). Like for the previous case, the scene
26 reveals an important amount of particles transported above clouds with an average ACAOT
27 (Fig. [8a](#)) of 0.31 and a peak at 3.0 southward of the Kamchatka Peninsula (latitude 50°). On
28 the northwest side of the peninsula, aerosol radii are found to be between 0.10 and 0.12 μm
29 and, on the other side, the retrieved [radii](#) are a bit larger (between 0.12 and 0.16 μm). In
30 parallel, slightly larger values of the angström exponent (Fig. [8b](#)) are found in the upper part
31 of the scene (mean value of 2.19) than southward (mean value of 2.02). Despite the fact that
32 aerosols have the same size as for the African event, the angström exponent reached higher

F. Peers 23/2/y 17:33
Supprimé: Figure 6f
F. Peers 23/2/y 17:33
Supprimé: very
F. Peers 23/2/y 17:33
Supprimé:),

F. Peers 23/2/y 17:33
Supprimé: due to
F. Peers 23/2/y 17:33
Supprimé: important
F. Peers 23/2/y 17:33
Supprimé: an important
F. Peers 23/2/y 17:33
Supprimé: The
F. Peers 23/2/y 17:33
Supprimé: of
F. Peers 23/2/y 17:33
Supprimé: 5b

F. Peers 23/2/y 17:33
Supprimé: Figure 7
F. Peers 23/2/y 17:33
Supprimé: 7a
F. Peers 23/2/y 17:33
Supprimé: models
F. Peers 23/2/y 17:33
Supprimé: 7b

1 values for the boreal emission. This is explained by the difference in the aerosol absorption
2 properties. The evaluated SSA (shown Fig. 8c) appears to be closer to 1.0 with a mean value
3 of 0.959 against 0.840 for the previous case study. It points out the scattering nature of the
4 boreal biomass burning aerosols compared to the African savannah ones, in accordance with
5 the study of Dubovik et al. [2002]. Moreover, one can also note the variability of the aerosol
6 absorption of this event: the northern part is associated not only to smallest particles, but also
7 to more absorbing particles with SSA of 0.943 (i.e. a mean complex refractive index of 0.008)
8 compared to 0.964 (respectively 0.005) in the south. [This difference may come from aerosol
9 aging: back trajectories suggest that air masses left inland Russia 3 days before arriving to the
10 Southern area while it took only 1 day to arrive in the Northern part of the plume.](#)

11 Like for the African biomass burning event, the ACCOT (Fig. 8d) is found to be in good
12 spatial agreement with the MODIS product. However, given the weak absorbing character of
13 the overlying aerosol layer, the biases between the two methods (Fig. 8e) are minimal. The
14 thickest clouds are associated with the largest MODIS underestimation (bias up to +12.0).
15 Moreover, one can also note the MODIS overestimation of the COT for thin cloud (bias up to
16 -10.7).

17 The evaluation of the DRE obtained for this event is presented in Fig. 8f. Large DRE are
18 observed in the northern part of the scene with values around 45 W.m^{-2} between 54 and 57°N .
19 On the opposite, the southwestern part (longitude lower than 160°E) is associated to large
20 negative DRE of about -50 W.m^{-2} . [As shown in Eq. \(1\), the sign of the perturbation depends
21 on the balance between the up-scattering and the absorption of the aerosol layer.](#) A warming
22 effect is expected where the aerosols are absorbing and the clouds are bright enough. On the
23 opposite, if the cloud is not optically thick (i.e. $\text{COT} < 10$) and the aerosols is scattering (SSA
24 close to 1), the particle layer enhances the albedo of the scene leading to a local cooling.
25 However, these large warming and cooling effects are spatially limited and 88% of the scene
26 have a DRE ranging from -30 to $+30 \text{ W.m}^{-2}$. On average, the radiative impact is almost
27 neutral with a mean DRE of about -3.5 W.m^{-2} .

28 4.1.3. Saharan dust

29 The last case study is related to a Saharan dust lifting that has been transported westward over
30 the Atlantic Ocean. These scenes are usually associated with high AOT values. The event of
31 the 4th of August 2008 off the coast of Morocco and Mauritania is not unique. In Fig. 9, we
32 report results for the two POLDER orbits (Fig. 6c). The western part, which is located in the

F. Peers 23/2/y 17:33

Supprimé: 7c

F. Peers 23/2/y 17:33

Supprimé: 7d

F. Peers 23/2/y 17:33

Supprimé: 7e

F. Peers 23/2/y 17:33

Supprimé: Figure 7f

F. Peers 23/2/y 17:33

Supprimé: 50 W.m^{-2} . Again, the approximate expression (Eq. 1) can clarify both situations.

F. Peers 23/2/y 17:33

Supprimé: Figure 8

F. Peers 23/2/y 17:33

Supprimé: 5c

1 core of a dust plume, has an average ACAOT (Fig. 9a) of 0.59 at 865 nm. The CALIOP
2 profile gives a cloud top altitude around 2 km and a dust layer at about 4 km. Dust detected
3 off the west coast of Morocco corresponds to a less intense event with a mean ACAOT of
4 0.27. It has to be remembered that we only retrieve the absorption of dust in the visible
5 (490 nm). Therefore we consider one model of aerosol absorption at 865 nm (i.e. complex
6 part of the refractive index fixed at 0.007), which corresponds to a SSA of 0.984 for this
7 wavelength. Thus, the angström exponent calculated (Fig. 9b) is constant over the scene and
8 is equal to 0.36. Regarding the absorption (Fig. 9c), the two events are again quite distinct. On
9 the one hand, the northern area is associated with SSA at 490 nm around 0.965 with a
10 complex part of the refractive index of 0.001. On the other hand, the western part is slightly
11 more absorbing with a mean SSA at 0.947 and a complex part of the refractive index around
12 0.002. These values are consistent with those reported by Dubovik et al. [2002].

13 Here again, the MODIS evaluation of the COT and our estimation (Fig. 9d) are close.
14 Moreover, the fact that dust does not strongly absorb at 865 nm (i.e. the wavelength used for
15 the MODIS retrieval of the COT) explains the small discrepancies observed between the two
16 methods (Fig. 9e) [Haywood et al., 2004]. However, MODIS overestimates the COT for more
17 than 60% of the scene with biases up to -5.3. As for the previous case, this is attributable to
18 the conjunction of thin clouds and scattering aerosols. On average, the bias is equal to -0.2.

19 Finally, the DRE of the scene has been processed (Fig. 9f). In contrast with the previous
20 cases, the presence of an aerosol layer above clouds results mostly in a cooling effect with a
21 negative DRE over 92% of the scene and an average value of -18.5 W.m^{-2} . The maximum
22 and minimum values of the radiative impact (respectively 41.3 and -91.9 W.m^{-2}) are reached
23 in the western area. One can also notice the correlation between retrieved ACCOT and the
24 DRE. Since the aerosol properties do not show a lot of variability there, it clearly illustrates
25 the influence of the cloud albedo on the calculation of the radiative impact. Thus, the correct
26 estimation of the COT has to be considered in order to accurately evaluate the radiative
27 impact of ACA.

28 4.2. Monthly DRE results over the South East Atlantic Ocean

29 The South East Atlantic Ocean is a preferential area to study aerosol interactions with clouds
30 and radiations because of the aerosol transport above clouds during the August-September dry
31 season. The impact of these biomass burning particles in cloudy scenes are expected to be
32 important not only locally, but also at wider scale through global-teleconnections [Jones et al.,

F. Peers 23/2/y 17:33

Supprimé: 8a

F. Peers 23/2/y 17:33

Supprimé: near-UV.

F. Peers 23/2/y 17:33

Supprimé: 8b

F. Peers 23/2/y 17:33

Supprimé: 8c

F. Peers 23/2/y 17:33

Supprimé: southern area

F. Peers 23/2/y 17:33

Supprimé: 8d) closely look alike.

F. Peers 23/2/y 17:33

Supprimé: a lot

F. Peers 23/2/y 17:33

Supprimé: 8e).

F. Peers 23/2/y 17:33

Supprimé: overestimate

F. Peers 23/2/y 17:33

Supprimé: 8f

F. Peers 23/2/y 17:33

Supprimé: noticed

1 2009; Jones and Haywood, 2012]. However, the radiative impact of aerosols for the South
2 West African coast remains uncertain for global aerosol models, starting with their direct
3 effect [Myhre et al., 2013a].

4 The aerosol and cloud properties have been evaluated over the South East Atlantic Ocean
5 during the fire season in August 2006. Important events of biomass burning aerosols over
6 clouds have been detected, especially between the 10th and 24th. The largest events (i.e. with
7 an ACAOT larger than 0.2) represent 28.9 % of the observed scenes. They are characterized
8 by strongly absorbing aerosols with a SSA of 0.867 at 865 nm. Then, the instantaneous
9 radiative forcing of aerosols above clouds has been computed. The monthly averaged DRE
10 values and the corresponding number of observations are reported in [Fig. 10a](#) and [10b](#)
11 respectively. Each pixel corresponds to 3 POLDER observations in the mean, with a
12 maximum at 13 observed events off the Angolan coast. As for the case study in August 2008
13 (Fig. 7), almost all ACA events lead to a warming effect. The maximum values are observed
14 near the coast close to 8°S latitude with averaged DRE around 125 W.m⁻², [which is consistent](#)
15 [with the study of De Graaf et al. \[2012\]](#).

16 Figure 11 displays the distribution of the DRE values reached during the month. First, it can
17 be noticed that about 14% of the observed scenes have a DRE between 0.0 and 2.5 W.m⁻². It
18 is important to remember that our method is highly sensitive to the scattering process thanks
19 to polarization measurements. Thus, we are able to well detect scenes with low AOT or with
20 weak absorption. Combined with thick clouds, these events lead to slightly positive DRE
21 values. In contrast, large warming effects have been observed, with DRE greater than
22 75 W.m⁻² over 12.7% of the scenes. Less than 0.2% of the pixels are even associated with
23 DRE larger than 220 W.m⁻². These dramatic values have been obtained for located high
24 loading of absorbing aerosols (i.e. AOT larger than 0.3 and SSA lower than 0.85 at 865 nm)
25 between [9](#) and [17 August](#). However, the estimation of the DRE for those intense events has to
26 be considered with caution since our estimation of the aerosol properties may be less accurate.
27 During the first part of the retrieval, we consider that the aerosol absorption does not impact
28 the polarized signal (Fig. 2). This assumption becomes questionable when the amount of
29 aerosols above clouds is very large. On the other hand, around 5% of the events have a
30 negative DRE with a minimum at -41.6 W.m⁻². The average DRE for August 2006 is 33.5
31 W.m⁻², which is of the same order of magnitude than the value obtained by De Graaf et al.
32 [2012] with SCIAMACHY measurements (i.e. 23 W.m⁻²). However, it has to be noted that
33 the two satellite instruments do not [observe](#) the scene at the same time. Changes of the scene

F. Peers 23/2/y 17:33

Supprimé: Figure 9a

F. Peers 23/2/y 17:33

Supprimé: 9b

F. Peers 23/2/y 17:33

Supprimé: 6

F. Peers 23/2/y 17:33

Supprimé: .

F. Peers 23/2/y 17:33

Supprimé: 10

F. Peers 23/2/y 17:33

Supprimé: the 9th

F. Peers 23/2/y 17:33

Supprimé: the 17th

F. Peers 23/2/y 17:33

Supprimé: observed

1 between the two measurements [Min et al., 2014] and the difference of solar zenith angles can
2 explain the remaining discrepancies. Furthermore, our algorithm is limited to optically thick
3 cloud ($COT > 3$) and cannot be applied to fractional cloud coverage.

4 5. Cloud heterogeneity effects

5 Our method assumes that clouds are horizontally and vertically homogeneous owing to the
6 use of plan-parallel radiative transfer algorithm (i.e. 1D code). However, lots of studies have
7 shown that the horizontal heterogeneity of clouds affects the scattered radiation measurements
8 through three-dimensional radiative transfer effects [e.g. Marshak and Davis, 2005; Cornet et
9 al., 2013; Zhang et al., 2012]. The cloud heterogeneity may thus affect our estimation of
10 aerosol and cloud properties as well as the DRE. To process the signal considering a more
11 realistic cloud field, a 3D radiative transfer code was used.

12 5.1. 3D modeling

13 In order to evaluate the impacts of cloud heterogeneities, the signal (i.e. radiances, polarized
14 radiances and fluxes) for one pixel of an ACA event has been modeled with the Monte-Carlo
15 radiative transfer code 3DMCPOL [Cornet et al., 2010]. The cloud field has been generated
16 using the algorithm 3DCLOUD [Szczap et al., 2014] and the heterogeneity controlled through
17 the inhomogeneity parameter $\rho = \sigma(COT) / COT$, where $\sigma(COT)$ is the standard deviation of
18 the COT within the pixel. It has to be noted that our algorithm include a filter on the cloud
19 heterogeneity that rejects pixels with $\sigma(COT)$ larger than 7.0. [To process the cloud field](#), the
20 inhomogeneity parameter ρ has been [fixed at 0.6](#), which represents a [standard value](#) for
21 stratocumulus clouds [Szczap et al., 2000a & 2000b]. [A statistical analysis of the](#)
22 [inhomogeneity parameter has been performed over the ACA scene sampled by the algorithm.](#)
23 [It shows that \$\rho = 0.6\$ can be considered has a high value in this study.](#) The mean COT has
24 been set to 10.0 and the cloud droplet size distribution is assumed to follow a lognormal
25 distribution with $r_{eff} = 11.0 \mu m$ and $v_{eff} = 0.02$. The overlying aerosol layer is composed of fine
26 mode particles with an effective radius of $0.12 \mu m$, an ACAOT of 0.142 at 865 nm and an
27 SSA of 0.781 (i.e. $k = 0.035$). The [Radiative Transfer \(RT\)](#) simulations [have](#) been made for a
28 solar incidence angle of 40° at the 3 wavelengths used for the retrievals and for a usual
29 POLDER angular configuration.

F. Peers 23/2/y 17:33

Supprimé: thanks to

F. Peers 23/2/y 17:33

Supprimé: A statistical analysis of

F. Peers 23/2/y 17:33

Supprimé: made on the ACA events we have studied and we have choose to fix $\rho = 0.6$

F. Peers 23/2/y 17:33

Supprimé: high value in our analysis but a

F. Peers 23/2/y 17:33

Supprimé: one

F. Peers 23/2/y 17:33

Supprimé: has

1 5.2. Effects on aerosol and cloud retrieved properties

2 The estimation of cloud and aerosol properties using our algorithm has been obtained from
3 the 3D modeled signal. As the horizontal heterogeneity of the cloud field influences weakly
4 the polarized signal, which is mostly sensitive to the first orders of scattering, the value of the
5 scattering AOT and the aerosol model retrieved during the first part of the method are not
6 affected.

7 On the contrary, the total radiances are strongly impacted by the cloud heterogeneity. The
8 total radiances modeled with 3DMCPOL are shown in [Fig. 12](#) as well as the ones modeled
9 with the 1D configuration with the mean cloud properties of the 3D fields. On average, the
10 plan-parallel cloud (i.e. 1D) produces [9.2% at 490 nm and 12.6% at 865 nm](#) more signal than
11 the heterogeneous cloud field. To a lesser extent, the angular behavior is also affected with a
12 more pronounced curve for the 3D modeled signal than for the 1D one. The overestimation
13 due to the 1D assumption influences both wavelengths and consequently the radiance ratio
14 L_{490}/L_{865} is less modified than the total signal. It is 94.1% for the homogeneous cloud and
15 97.0% for the heterogeneous one. The aerosol SSA, which is principally sensitive to the
16 radiance ratio, is thus not too much impacted by the 3D effects contrary to the retrieved value
17 of the ACCOT. Using a 1D assumption, the aerosol absorption is slightly underestimated with
18 an SSA of 0.794 ($k = 0.0325$) instead of 0.781 at 865 nm. Therefore, the retrieved AOT is also
19 a little smaller than the expected one (i.e. 0.140 instead of 0.142 at 865 nm). In parallel, our
20 method evaluates the COT at 7.6, which corresponds to an underestimation of 24%
21 comparing to the mean value (i.e. 10.0).

22 5.3. Effect on the DRE

23 In the same way that 3D effects influence radiances, fluxes are expected to vary with the
24 heterogeneity of clouds. The quantification of the DRE of aerosols for realistic heterogeneous
25 cloud scene would need 3D radiative transfer modeling of the fluxes, which is too time
26 consuming. To evaluate the error on the DRE due to the homogeneous cloud assumption, we
27 compare the differences between, on the one hand, the 3D TOA fluxes with and without
28 aerosols for the case described in the previous section and, on the other hand, 1D TOA fluxes
29 with the 1D-equivalent aerosol and cloud properties (i.e. $COT = 7.6$; $AOT_{865nm} = 0.140$;
30 $k = 0.0325$). For computing time reason, the analysis focus on fluxes processed at 490 nm.

31 The results obtained from both modeling are shown in [Table 2](#). The fluxes computed with the

F. Peers 23/2/y 17:33

Supprimé: Figure 11

F. Peers 23/2/y 17:33

Supprimé: 11%

F. Peers 23/2/y 17:33

Supprimé: 4

1 1D assumption, which corresponds to the one obtained with our method, is close to the ones
2 given by the 3D modeling (underestimation lower than 2.5%). We can also note that the
3 difference between 3D and 1D modeling is smaller for the polluted cloud scene than for the
4 clean cloud, which means that the aerosols tend to smooth the underneath cloud
5 heterogeneity. The exact $DRE_{0.490\mu m}$ (i.e. computed with the 3D modeling) is equal to 92.06
6 $W.m^{-2}.\mu m^{-1}$ while we have obtained $81.92 W.m^{-2}.\mu m^{-1}$ with the 1D assumption. Therefore,
7 considering a plan-parallel cloud for both retrieval and DRE processing leads to slightly
8 underestimate the radiative impact of aerosols, in case of cloud heterogeneity. For the scenes
9 presented in this paper (i.e. which meet our selection criteria), the obtained values can be seen
10 as a lower bound for the ACA DRE. Finally, let us mention that this error is expected to be
11 smaller at higher wavelength and consequently for the solar DRE since the effect of aerosol
12 absorption is the largest in the UV.

13 6. Conclusion

14 In this study, we introduced a new approach for the retrieval of aerosol and cloud properties
15 (i.e. AOT, SSA and COT) when an aerosol layer is overlying a liquid cloud above the ocean.
16 Its range of application is restricted to homogeneous clouds with COT larger than 3. The
17 strong point of the algorithm is to combine the sensitivity provided by both total and polarized
18 measurements from the passive satellite instrument POLDER. In a first step, the information
19 on the scattering state of the aerosol layer is given by polarized radiances. The presence of an
20 aerosol layer above a thick liquid cloud leads to a significant enhancement of the polarization
21 at side scattering angle that is used to retrieve the scattering AOT and the aerosol size. Then,
22 these properties together with total radiances are used to determine simultaneously the
23 absorption of the aerosol layer and the COT. In that way, this method allows retrieving the
24 aerosol layer properties with minimum assumptions and the cloud properties corrected from
25 the aerosol absorption.

26 Nevertheless, the impact of the approximations and the assumptions of the method have been
27 assessed. The largest incertitude about the SSA is due to the approximation about the weak
28 sensitivity of polarized radiances to absorption. When the aerosol size distribution is
29 dominated by the fine mode, an underestimation of -0.055 can be expected for extreme event
30 of absorbing aerosols above clouds (i.e. $AOT_{865nm} = 0.6$ and $SSA_{865nm} = 0.77$). Otherwise, the
31 bias on the SSA is below 0.03. It has to be pointed out that the underestimation of the SSA
32 always goes together with an underestimation of the scattering AOT. As a consequence, the

F. Peers 23/2/y 17:33

Supprimé: . The values

F. Peers 23/2/y 17:33

Supprimé: method

1 [algorithm presented here provides a reliable estimation of the absorption AOT, which is](#)
2 [among the most important parameters to evaluate the DRE of aerosols above clouds.](#)

3 The algorithm has shown its ability to retrieve aerosol and cloud properties for three case
4 studies with very different characteristics. The first one is related to a biomass burning event
5 off the South West African coast, which is a scene frequently used for ACA studies. As
6 expected, these aerosols are found to be [strongly](#) absorbing with SSA of 0.84 at 865 nm.
7 Moreover, the COT given by MODIS is largely underestimated over the scene, which
8 highlights the importance of taking into account the absorption of aerosol for the COT
9 retrieval. The second example is devoted to Siberian biomass burning. It illustrates the high
10 variability of ACA properties with an average particle SSA at 0.96. In contrast with the
11 previous scene, the enhancement of scattering due to these aerosols may cause an
12 overestimation of the COT by MODIS. Finally, the algorithm can be used not only on fine
13 mode aerosols above clouds, but also on dust particles. The study of Saharan dust transported
14 over clouds has revealed the ability of the method to evaluate the differential dust absorption
15 of visible light at short wavelength for a given value at 865 nm. It should be added that low
16 differences [have](#) been observed between our COT retrieval and the MODIS one where the
17 AOT is the smallest. Such biases have already been observed by Zeng et al. [2012] and are
18 primarily due to the difference of instrument characteristics.

19 Furthermore, we developed a procedure to evaluate the DRE of aerosols above clouds based
20 on exact calculations. The radiative impact processed for the three case studies confirms the
21 need of accurately quantifying the aerosol absorption and the brightness of the underneath
22 cloud. Thick clouds in association with [highly](#) absorbing aerosols translate into a warming
23 effect and can reach high DRE values as for the African biomass burning aerosols. On the
24 opposite, a cooling effect can be observed for scenes with low aerosol absorption and thin
25 clouds as for the Saharan dust event. The estimated DRE for Siberian biomass burning
26 aerosols is spatially contrasting since both cloud and aerosol properties show variability.

27 The algorithm has been applied [to](#) one month of measurements over the South East Atlantic
28 Ocean. August 2006 is characterized by important amount of absorbing biomass burning
29 aerosols above the permanent stratocumulus deck. The DRE has been processed. The
30 presence of the aerosol layer above bright clouds is responsible for a large radiative impact.
31 The monthly averaged value over the scene is estimated at 33.5 W.m^{-2} , which is [of the same](#)
32 [order of magnitude as the estimation of De Graaf et al. \[2012\] \(i.e. \$23 \text{ W.m}^{-2}\$ \). Let us point out](#)
33 [that differences between the result of this study and the literature are expected and are mainly](#)

F. Peers 23/2/y 17:33
Supprimé: accurately

F. Peers 23/2/y 17:33
Supprimé: very

F. Peers 23/2/y 17:33
Supprimé: has

F. Peers 23/2/y 17:33
Supprimé: very

F. Peers 23/2/y 17:33
Supprimé: on

F. Peers 23/2/y 17:33
Supprimé: comparable to the one given by De Graaf et al. [2012]. This analysis shows how important the studies of ACA are for the climate understanding.

1 [due to the selection of the AAC scenes: this analysis does not include thin clouds \(i.e.](#)
2 [COT < 3\) and scene with fractional cloud coverage which leads to biased high the DRE.](#) The
3 algorithm developed here could provide aerosol and cloud properties that can be used to better
4 constrain numerical models, leading to a reduction of their uncertainty.

5 Some efforts still have to be done to enhance our knowledge on aerosols above clouds.
6 Currently, the described method allows the retrieval of aerosol and cloud properties only over
7 the ocean. The procedure has to be extended to ACA events over land, which requires paying
8 attention to the contribution of the surface to the measurements. Another key point is the
9 study of aerosols over thin layer of clouds. The first part of the algorithm relies on the
10 independence of the polarized signal for optically thick clouds. To go further, scenes with
11 aerosols in fractional cloud coverage have to be investigated. The cloud inhomogeneity also
12 affects the radiances and fluxes of ACA scenes. Thus, we have examined the impact of
13 considering a plan-parallel cloud on the aerosol and cloud properties as well as the DRE. On
14 the one hand, the retrieval of aerosol properties is weakly biased since polarized radiances and
15 radiance ratio are not significantly affected by cloud heterogeneity. Finally, the homogeneous
16 cloud assumption leads to [an underestimation of the DRE of aerosols. This bias remains small](#)
17 [in this study because scenes with too heterogeneous clouds are rejected. However, a thorough](#)
18 [analysis of the effect of the homogeneous cloud assumption on the estimation of the DRE](#)
19 [would provide a significant contribution to the scientific field.](#)

20 The first results obtained for ACA scenes over the ocean are promising and confirms the need
21 of both global and temporal distribution aerosol and cloud properties. Thus, our next target
22 will be to analyze POLDER measurements over the whole database and to give a first
23 estimation of the global DRE of aerosols over cloudy skies.

24 **Acknowledgements**

25 This work has been supported by the Programme National de Télédétection Spatiale (PNTS,
26 <http://www.insu.cnrs.fr/pnts>), grant n° PNTS-2013-10 and n° PNTS-2014-02. The authors are
27 grateful to CNES, NASA, and the ICARE data and services center.

28 The authors acknowledge the support of France Grilles for providing computing resources on
29 the French National Grid Infrastructure.

F. Peers 23/2/y 17:33

Supprimé: On the other hand, 3D effects cause bias on our estimation of the COT.

F. Peers 23/2/y 17:33

Supprimé: a slight

F. Peers 23/2/y 17:33

Supprimé: actions-sur-projets/pnts-programme-national-de-teledetection-spatiale

1 The authors would like to thank the reviewers for their valuable comments and suggestions
2 that considerably improved the article. Finally, they are grateful to the editor, Paola Formenti,
3 for her help during the editorial process.
4

1 References

- 2 Ackerman, A. S., Toon, O. B., Stevens, D. E., Heymsfield, A. J., Ramanathan, V., & Welton,
3 E. J. (2000). Reduction of tropical cloudiness by soot. *Science*, 288(5468), 1042-1047.
- 4 Albrecht, B. A. (1989). Aerosols, cloud microphysics, and fractional
5 cloudiness. *Science*, 245(4923), 1227-1230.
- 6 Balkanski, Y., Schulz, M., Claquin, T., & Guibert, S. (2007). Reevaluation of Mineral aerosol
7 radiative forcings suggests a better agreement with satellite and AERONET
8 data. *Atmospheric Chemistry and Physics*, 7(1), 81-95.
- 9 Bréon, F. M., Tanré, D., & Generoso, S. (2002). Aerosol effect on cloud droplet size
10 monitored from satellite. *Science*, 295(5556), 834-838.
- 11 Chakrabarty, R. K., Moosmüller, H., Chen, L. W., Lewis, K., Arnott, W. P., Mazzoleni, C.,
12 Dubey, M. K., Wold, C. E., Hao, W. M., & Kreidenweis, S. M. (2010). Brown carbon
13 in tar balls from smoldering biomass combustion. *Atmospheric Chemistry and
14 Physics*, 10(13), 6363-6370.
- 15 Chand, D., Anderson, T. L., Wood, R., Charlson, R. J., Hu, Y., Liu, Z., & Vaughan, M.
16 (2008). Quantifying above-cloud aerosol using spaceborne lidar for improved
17 understanding of cloudy-sky direct climate forcing. *Journal of Geophysical Research:
18 Atmospheres (1984–2012)*, 113, [D13206](#), doi: [10.1029/2007JD009433](#).
- 19 Chand, D., Wood, R., Anderson, T. L., Satheesh, S. K., & Charlson, R. J. (2009). Satellite-
20 derived direct radiative effect of aerosols dependent on cloud cover. *Nature
21 Geoscience*, 2(3), 181-184.
- 22 Coddington, O. M., Pilewskie, P., Redemann, J., Platnick, S., Russell, P. B., Schmidt, K. S.,
23 & Vukicevic, T. (2010). Examining the impact of overlying aerosols on the retrieval of
24 cloud optical properties from passive remote sensing. *Journal of Geophysical Research:
25 Atmospheres (1984–2012)*, 115, [D10211](#), doi: [10.1029/2009JD012829](#).
- 26 Cole, A. E., Court, A., & Kantor, A.J. (1965). Model atmospheres. *Handbook of geophysics
27 and space environment*, in: Chap. 2, edited by: Valley, S. L., McGraw-Hill, New York,
28 [1965](#).
- 29 Cornet, C., Labonnote, L. C. and Szczap, F. (2010). Three-dimensional polarized Monte
30 Carlo atmospheric radiative transfer model (3DMCPOL): 3D effects on polarized

F. Peers 23/2/y 17:33

Supprimé: (D13).

F. Peers 23/2/y 17:33

Supprimé: (D10).

F. Peers 23/2/y 17:33

Supprimé: .

1 visible reflectances of a cirrus cloud. *Journal of Quantitative Spectroscopy and*
 2 *Radiative Transfer*, 111(1), 174-186.

3 Cornet, C., Szczap, F., Labonnote, L. C., Fauchez, T., Parol, F., Thieuleux, F., Riedi, J.,
 4 Dubuisson, P., & Ferlay, N. (2013). Evaluation of cloud heterogeneity effects on total
 5 and polarized visible radiances as measured by POLDER/PARASOL and consequences
 6 for retrieved cloud properties. In *RADIATION PROCESSES IN THE ATMOSPHERE*
 7 *AND OCEAN (IRS2012): Proceedings of the International Radiation Symposium*
 8 *(IRC/IAMAS)* (Vol. 1531, No. 1, pp. 99-102). AIP Publishing.

9 Costantino, L., & Bréon, F. M. (2013). Satellite-based estimate of aerosol direct radiative
 10 effect over the South-East Atlantic. *Atmospheric Chemistry and Physics*
 11 *Discussions*, 13(9), 23295-23324.

12 Cox, C., & Munk, W. (1954). Measurement of the roughness of the sea surface from
 13 photographs of the sun's glitter. *JOSA*, 44(11), 838-850.

14 De Graaf, M., Tilstra, L. G., Wang, P., & Stammes, P. (2012). Retrieval of the aerosol direct
 15 radiative effect over clouds from spaceborne spectrometry. *Journal of Geophysical*
 16 *Research: Atmospheres (1984–2012)*, 117, [D07207](#), doi:10.1029/2011JD017160.

17 De Haan, J. F., Bosma, P. B., & Hovenier, J. W. (1987). The adding method for multiple
 18 scattering calculations of polarized light. *Astronomy and Astrophysics*, 183, 371-391.

19 Deuzé, J. L., Herman, M., & Santer, R. (1989). Fourier series expansion of the transfer
 20 equation in the atmosphere-ocean system. *Journal of Quantitative Spectroscopy and*
 21 *Radiative Transfer*, 41(6), 483-494.

22 Dubuisson P., J.-C. Roger, M. Mallet, O. Dubovik, a code to compute the direct solar
 23 radiative forcing: application to anthropogenic aerosols during the Escompte
 24 experiment, Proceedings of IRS 2004: Current Problems in Atmospheric Radiation, [23–](#)
 25 [28 August 2004](#), Busan, [Korea](#), 2004.

26 Dubovik, O., Holben, B., Eck, T. F., Smirnov, A., Kaufman, Y. J., King, M. D., Tanré, D., &
 27 Slutsker, I. (2002). Variability of absorption and optical properties of key aerosol types
 28 observed in worldwide locations. *Journal of the Atmospheric Sciences*, 59, [590–608](#),
 29 [doi:10.1175/1520-0469\(2002\)059<0590:VOAAOP>2.0.CO;2, 2002](#).

30 Fougnie, B., Bracco, G., Lafrance, B., Ruffel, C., Hagolle, O., & Tinel, C. (2007). PARASOL
 31 in-flight calibration and performance. *Applied optics*, 46(22), 5435-5451.

F. Peers 23/2/y 17:33

Supprimé: (D7).

F. Peers 23/2/y 17:33

Supprimé: august

F. Peers 23/2/y 17:33

Supprimé: (3).

- 1 Giglio, L., Descloitres, J., Justice, C. O., & Kaufman, Y. J. (2003). An enhanced contextual
2 fire detection algorithm for MODIS. *Remote sensing of environment*, 87(2), 273-282.
- 3 Hasekamp, O. P.: Capability of multi-viewing-angle photo-polarimetric measurements for the
4 simultaneous retrieval of aerosol and cloud properties. *Atmospheric Measurement*
5 *Techniques*, 3, 839–851, doi:10.5194/amt-3-839-2010, 2010.
- 6 Haywood, J. M., Osborne, S. R., & Abel, S. J. (2004). The effect of overlying absorbing
7 aerosol layers on remote sensing retrievals of cloud effective radius and cloud optical
8 depth. *Quarterly Journal of the Royal Meteorological Society*, 130(598), 779-800.
- 9 Herman, M., Deuzé, J. L., Marchand, A., Roger, B., & Lallart, P. (2005). Aerosol remote
10 sensing from POLDER/ADEOS over the ocean: Improved retrieval using a
11 nonspherical particle model. *Journal of Geophysical Research: Atmospheres* (1984–
12 2012), 110, D10S02, doi:10.1029/2004JD004798.
- 13 Hu, Y., Vaughan, M., Liu, Z., Powell, K., & Rodier, S. (2007). Retrieving optical depths and
14 lidar ratios for transparent layers above opaque water clouds from CALIPSO lidar
15 measurements. *Geoscience and Remote Sensing Letters, IEEE*, 4(4), 523-526.
- 16 Jaffe, D., Bertschi, I., Jaeglé, L., Novelli, P., Reid, J. S., Tanimoto, H., Vingarzan, R., &
17 Westphal, D. L. (2004). Long-range transport of Siberian biomass burning emissions
18 and impact on surface ozone in western North America. *Geophysical Research*
19 *Letters*, 31, L16106, doi:10.1029/2004GL020093.
- 20 Jethva, H., Torres, O., Remer, L. A., & Bhartia, P. K. (2013). A color ratio method for
21 simultaneous retrieval of aerosol and cloud optical thickness of above-cloud absorbing
22 aerosols from passive sensors: Application to MODIS measurements. *IEEE T. Geosci.*
23 *Remote Sens*, 51, 3862–3870, 2013.
- 24 Jethva, H., Torres, O., Waquet, F., Chand, D., & Hu, Y. (2014). How do A-train sensors
25 intercompare in the retrieval of above-cloud aerosol optical depth? A case study-based
26 assessment. *Geophysical Research Letters*, 41, 186–192, doi:10.1002/2013GL058405,
27 2014.
- 28 Johnson, B. T., Shine, K. P., & Forster, P. M. (2004). The semi-direct aerosol effect: Impact
29 of absorbing aerosols on marine stratocumulus. *Quarterly Journal of the Royal*
30 *Meteorological Society*, 130(599), 1407-1422.

F. Peers 23/2/y 17:33

Supprimé: (2010).

F. Peers 23/2/y 17:33

Supprimé: .

F. Peers 23/2/y 17:33

Supprimé: Discussions,

F. Peers 23/2/y 17:33

Supprimé: (2), 1229-1262

F. Peers 23/2/y 17:33

Supprimé: (D10).

F. Peers 23/2/y 17:33

Supprimé: (16).

- 1 | [Johnson, B. T., Osborne, S. R., Haywood, J. M., & Harrison, M. A. J. \(2008\). Aircraft](#)
2 | [measurements of biomass burning aerosol over West Africa during DABEX. *Journal of*](#)
3 | [Geophysical Research: Atmospheres \(1984–2012\), 113\(D23\).](#)
- 4 | Jones, A., Haywood, J., & Boucher, O. (2009). Climate impacts of geoengineering marine
5 | stratocumulus clouds. *Journal of Geophysical Research: Atmospheres (1984–*
6 | *2012)*, 114, [D10106](#), doi:10.1029/2008JD011450.
- 7 | Jones, A., & Haywood, J. M. (2012). Sea-spray geoengineering in the HadGEM2-ES earth-
8 | system model: radiative impact and climate response. *Atmospheric Chemistry and*
9 | *Physics*, 12(22), 10887-10898.
- 10 | Kaufman, Y. J., Koren, I., Remer, L. A., Rosenfeld, D., & Rudich, Y. (2005). The effect of
11 | smoke, dust, and pollution aerosol on shallow cloud development over the Atlantic
12 | Ocean. *Proceedings of the National Academy of Sciences of the United States of*
13 | *America*, 102(32), 11207-11212.
- 14 | Kirchstetter, T. W., Novakov, T., & Hobbs, P. V. (2004). Evidence that the spectral
15 | dependence of light absorption by aerosols is affected by organic carbon. *Journal of*
16 | *Geophysical Research: Atmospheres (1984–2012)*, 109, [D21208](#), doi:10.1029/
17 | [2004JD004999](#).
- 18 | Knobelspiesse, K., Cairns, B., Redemann, J., Bergstrom, R. W., & Stohl, A. (2011).
19 | Simultaneous retrieval of aerosol and cloud properties during the MILAGRO field
20 | campaign. *Atmospheric Chemistry and Physics*, 11(13), 6245-6263.
- 21 | Koren, I., Kaufman, Y. J., Remer, L. A., & Martins, J. V. (2004). Measurement of the effect
22 | of Amazon smoke on inhibition of cloud formation. *Science*, 303(5662), 1342-1345.
- 23 | Leahy, L. V., Anderson, T. L., Eck, T. F., & Bergstrom, R. W. (2007). A synthesis of single
24 | scattering albedo of biomass burning aerosol over southern Africa during SAFARI
25 | 2000. *Geophysical Research Letters*, 34, [L12814](#), doi:10.1029/2007GL029697.
- 26 | Lee, K. H., Kim, J. E., Kim, Y. J., Kim, J., & von Hoyningen-Huene, W. (2005). Impact of
27 | the smoke aerosol from Russian forest fires on the atmospheric environment over Korea
28 | during May 2003. *Atmospheric Environment*, 39(1), 85-99.
- 29 | Lenoble, J., Tanré, D., Deschamps, P. Y., & Herman, M. (1982). A simple method to
30 | compute the change in earth-atmosphere radiative balance due to a stratospheric aerosol
31 | layer. *Journal of the Atmospheric Sciences*, 39(11), 2565-2576.

F. Peers 23/2/y 17:33

Supprimé: (D10).

F. Peers 23/2/y 17:33

Supprimé: (D21).

F. Peers 23/2/y 17:33

Supprimé: (12).

- 1 Marshak, A., & Davis, A. (Eds.). (2005). *3D Radiative Transfer in Cloudy Atmospheres* (Vol.
2 5117). Springer, [Berlin, Heidelberg, 2005](#).
- 3 Meyer, K., Platnick, S., Oreopoulos, L., & Lee, D. (2013). Estimating the direct radiative
4 effect of absorbing aerosols overlying marine boundary layer clouds in the southeast
5 Atlantic using MODIS and CALIOP. *Journal of Geophysical Research:
6 Atmospheres*, *118*(10), 4801-4815.
- 7 Min, M., & Zhang, Z. (2014). On the influence of cloud fraction diurnal cycle and sub-grid
8 cloud optical thickness variability on all-sky direct aerosol radiative forcing. *Journal of
9 Quantitative Spectroscopy and Radiative Transfer*, *142*, 25-36.
- 10 Myhre, G., Samset, B. H., Schulz, M., Balkanski, Y., Bauer, S., Berntsen, T. K., Bian, H.,
11 Bellouin, N., Chin, M., Diehl, T., Easter, R. C., Feichter, J., Ghan, S. J., Hauglustaine,
12 D., Iversen, T., Kinne, S., Kirkevåg, A., Lamarque, J.-F., Lin, G., Liu, X., Lund, M. T.,
13 Luo, G., Ma, X., van Noije, T., Penner, J. E., Rasch, P. J., Ruiz, A., Seland, Ø., Skeie,
14 R. B., Stier, P., Takemura, T., Tsigaridis, K., Wang, P., Xu, L., Yu, H., Yoon, J.-F.,
15 Zhang, H., & Zhou, C. (2013a). Radiative forcing of the direct aerosol effect from
16 AeroCom Phase II simulations. *Atmospheric Chemistry & Physics*, *13*(4).
- 17 Myhre, G., D. Shindell, F.-M. Bréon, W. Collins, J. Fuglestedt, J. Huang, D. Koch, J.-F.
18 Lamarque, D. Lee, B. Mendoza, T. Nakajima, A. Robock, G. Stephens, T. Takemura
19 and H. Zhang, 2013: Anthropogenic and Natural Radiative Forcing. In: Climate Change
20 2013: The Physical Science Basis. Contribution of Working Group I to the Fifth
21 Assessment Report of the Intergovernmental Panel on Climate Change, edited by:
22 Stocker, T.F., D. Qin, G.-K. Plattner, M. Tignor, S.K. Allen, J. Boschung, A. Nauels, Y.
23 Xia, V. Bex and P.M. Midgley, Cambridge University Press, Cambridge, UK and New
24 York, NY, USA, 571-657, 2013b
- 25 Nakajima, T., & King, M. D. (1990). Determination of the optical thickness and effective
26 particle radius of clouds from reflected solar radiation measurements. Part I:
27 Theory. *Journal of the atmospheric sciences*, *47*(15), 1878-1893.
- 28 Paris, J. D., Stohl, A., Nédélec, P., Arshinov, M. Y., Panchenko, M. V., Shmargunov, V. P.,
29 Law, K. S., Belan, B. D., & Ciais, P. (2009). Wildfire smoke in the Siberian Arctic in
30 summer: source characterization and plume evolution from airborne
31 measurements. *Atmospheric Chemistry and Physics*, *9*(23), 9315-9327.

- 1 Péré, J. C., Bessagnet, B., Mallet, M., Waquet, F., Chiapello, I., Minvielle, F., Pont, V., &
2 Menut, L. (2014). Direct radiative effect of the Russian wildfires and its impact on air
3 temperature and atmospheric dynamics during August 2010. *Atmospheric Chemistry
4 and Physics*, 14(4), 1999-2013.
- 5 Peters, K., Quaas, J., & Bellouin, N. (2011). Effects of absorbing aerosols in cloudy skies: a
6 satellite study over the Atlantic Ocean. *Atmospheric Chemistry and Physics*, 11(4),
7 1393-1404.
- 8 Ramanathan, V., Crutzen, P. J., Kiehl J. T., & Rosenfeld D. (2001). Aerosols, climate, and the
9 hydrological cycle. *Science*, 294(5549), 2119-2124.
- 10 Rossow, W. B., Garder, L. C., & Lacis, A. A. (1989). Global, seasonal cloud variations from
11 satellite radiance measurements. Part I: Sensitivity of analysis. *Journal of Climate*, 2(5),
12 419-458.
- 13 [Sayer, A. M., Hsu, N. C., Eck, T. F., Smirnov, A., & Holben, B. N. \(2014\). AERONET-based
14 models of smoke-dominated aerosol near source regions and transported over oceans,
15 and implications for satellite retrievals of aerosol optical depth. *Atmospheric Chemistry
16 and Physics*, 14\(20\), 11493-11523.](#)
- 17 Stocks, B. J., Wotton, B. M., Flannigan, M. D., Fosberg, M. A., Cahoon, D. R., &
18 Goldammer, J. G. (2001). Boreal forest fire regimes and climate change. *Remote
19 Sensing and Climate Modeling: Synergies and Limitations* (pp. 233-246). Springer
20 Netherlands.
- 21 Szczap, F., Isaka, H., Saute, M., Guillemet, B., & Gour, Y. (2000a). Inhomogeneity effects of
22 1D and 2D bounded cascade model clouds on their effective radiative
23 properties. *Physics and Chemistry of the Earth, Part B: Hydrology, Oceans and
24 Atmosphere*, 25(2), 83-89.
- 25 Szczap, F., Isaka, H., Saute, M., Guillemet, B., & Ioltukhovski, A. (2000b). Effective
26 radiative properties of bounded cascade nonabsorbing clouds: Definition of the
27 equivalent homogeneous cloud approximation. *Journal of Geophysical Research:
28 Atmospheres (1984–2012)*, 105(D16), 20617-20633.
- 29 Szczap, F., Gour, Y., Fauchez, T., Cornet, C., Faure, T., Jourdan, O., [Penide, G., and Dubuis-
30 son, P.](#): A flexible three-dimensional stratocumulus, cumulus and cirrus cloud generator
31 (3DCLOUD) based on drastically simplified atmospheric equations and [the](#) Fourier

F. Peers 23/2/y 17:33

Supprimé: & Dubuisson, P. (2014).

1 transform framework, *Geoscience Model Development*, 7, 1779–1801,
 2 doi:10.5194/gmd-7-1779-2014, 2014.

3 Tanré, D., Bréon, F. M., Deuzé, J. L., Dubovik, O., Ducos, F., François, P., Goloub, P.,
 4 Herman, M., Lifermann, A., & Waquet, F. (2011). Remote sensing of aerosols by using
 5 polarized, directional and spectral measurements within the A-Train: the PARASOL
 6 mission. *Atmospheric Measurement Techniques*, 4(7), 1383-1395.

7 Torres, O., Jethva, H., & Bhartia, P. K. (2012). Retrieval of Aerosol Optical Depth above
 8 Clouds from OMI Observations: Sensitivity Analysis and Case Studies. *Journal of the
 9 Atmospheric Sciences*, 69, 1037–1053, doi: 10.1175/JAS-D-11-0130.1.

10 Twomey, S. (1974). Pollution and the planetary albedo. *Atmospheric Environment
 11 (1967)*, 8(12), 1251-1256.

12 Twomey, S. (1977). The influence of pollution on the shortwave albedo of clouds. *Journal of
 13 the Atmospheric Sciences*, 34(7), 1149-1152.

14 Vanbauce, C., Cadet, B., & Marchand, R. T. (2003). Comparison of POLDER apparent and
 15 corrected oxygen pressure to ARM/MMCR cloud boundary pressures. *Geophysical
 16 Research Letters*, 30, 1212, doi:10.1029/2002GL016449.

17 Waquet, F., Riedi, J., Labonnote, L. C., Goloub, P., Cairns, B., Deuzé, J. L., & Tanré, D.
 18 (2009). Aerosol Remote Sensing over Clouds Using A-Train Observations. *Journal of
 19 the Atmospheric Sciences*, 66, 2468–2480, doi: 10.1175/2009JAS3026.1.

20 Waquet, F., Cornet, C., Deuzé, J. L., Dubovik, O., Ducos, F., Goloub, P., Herman, M.,
 21 Lapyonok, T., Labonnote, L., C., & Vanbauce, C. (2013a). Retrieval of aerosol
 22 microphysical and optical properties above liquid clouds from POLDER/PARASOL
 23 polarization measurements. *Atmospheric Measurement Techniques*, 6(4), 991-1016.

24 Waquet, F., Peers, F., Ducos, F., Goloub, P., Platnick, S., Riedi, J., Tanré, D., & Thieuleux, F.
 25 (2013b). Global analysis of aerosol properties above clouds. *Geophysical Research
 26 Letters*, 40(21), 5809-5814.

27 Wilcox, E. M., & Platnick, S. (2009). Estimate of the impact of absorbing aerosol over cloud
 28 on the MODIS retrievals of cloud optical thickness and effective radius using two
 29 independent retrievals of liquid water path. *Journal of Geophysical Research:
 30 Atmospheres (1984–2012)*, 114, D05210, doi:10.1029/2008JD010589.

31 Winker, D. M., Vaughan, M. A., Omar, A., Hu, Y., Powell, K. A., Liu, Z., Hunt, W., &
 32 Young, S. A. (2009). Overview of the CALIPSO mission and CALIOP data processing

F. Peers 23/2/y 17:33

Supprimé: . Geoscientific

F. Peers 23/2/y 17:33

Supprimé: Discussions,

F. Peers 23/2/y 17:33

Supprimé: 295-337

F. Peers 23/2/y 17:33

Supprimé: (3).

F. Peers 23/2/y 17:33

Supprimé: (5).

F. Peers 23/2/y 17:33

Supprimé: (8).

F. Peers 23/2/y 17:33

Supprimé: (D5).

1 algorithms. *Journal of Atmospheric & Oceanic Technology*, 26, 2310–2323, doi:
2 [10.1175/2009JTECHA1281.1](https://doi.org/10.1175/2009JTECHA1281.1).

3 Winker, D. M., Tackett, J. L., Getzewich, B. J., Liu, Z., Vaughan, M. A., & Rogers, R. R.
4 (2013). The global 3-D distribution of tropospheric aerosols as characterized by
5 CALIOP. *Atmospheric Chemistry and Physics*, 13(6), 3345-3361.

6 Young, S. A., & Vaughan, M. A. (2009). The retrieval of profiles of particulate extinction
7 from Cloud-Aerosol Lidar Infrared Pathfinder Satellite Observations (CALIPSO) data:
8 Algorithm description. *Journal of Atmospheric & Oceanic Technology*, 26, 1105–1119,
9 doi: [10.1175/2008JTECHA1221.1](https://doi.org/10.1175/2008JTECHA1221.1).

10 Zeng, S., Cornet, C., Parol, F., Riedi, J., & Thieuleux, F. (2012). A better understanding of
11 cloud optical thickness derived from the passive sensors MODIS/AQUA and
12 POLDER/PARASOL in the A-Train constellation. *Atmospheric Chemistry and
13 Physics*, 12(23), 11245-11259.

14 Zhang, Y. H., Wooster, M. J., Tutubalina, O., & Perry, G. L. W. (2003). Monthly burned area
15 and forest fire carbon emission estimates for the Russian Federation from SPOT
16 VGT. *Remote Sensing of Environment*, 87(1), 1-15.

F. Peers 23/2/y 17:33

Supprimé: (11).

F. Peers 23/2/y 17:33

Supprimé: (6).

	Polarized LUT	Total radiance LUT
Aerosols models		
Vertical distribution	gaussian layer with a mean altitude of 3 km	homogeneous layer between 2 and 3 km
<u>Fine mode:</u>		
Size distribution	lognormal distribution with $\sigma_f = 0.4$ $r_{eff} = 0.06$ to $0.16 \mu\text{m}$ (by $0.02 \mu\text{m}$ step)	
Refractive index	1.47 – i.0.01	1.47 – i.k with k = 0.00 to 0.05 (by 0.0025 step)
<u>Dust:</u>		
Size distribution	bimodal lognormal distribution with $\sigma_f = 0.4$ $r_{eff, fine} = 0.35 \mu\text{m}$ $r_{eff, coarse} = 2.55 \mu\text{m}$	
Refractive index	1.47 – i.0.0007	1.47 – i.k $k_{865\text{nm}} = 0.0007$ $k_{490\text{nm}} = 0.0$ to 0.004 (by 0.0005 step)
Cloud models		
Vertical distribution	homogeneous layer from 0 to 0.75 km	homogeneous layer from 0 to 1 km
Size distribution	gamma law with $v_{eff} = 0.06$ $r_{eff} = 5$ to $26 \mu\text{m}$ (by $1 \mu\text{m}$ step)	
Refractive index		$r_{eff} = 10 \mu\text{m}$ $m_{r,490\text{nm}} = 1.338$ $m_{r,670\text{nm}} = 1.331$ $m_{r,865\text{nm}} = 1.330$

1 **Table 1.** Aerosol and cloud model properties used to compute the polarized and total radiance LUT of the POLDER
2 algorithm.

	3D modeling	1D modeling	(F _{1D} -F _{3D})/F _{3D} (%)
$F_{cloud+aer}^{\uparrow}$	569.01	564.48	-0.79
F_{cloud}^{\uparrow}	661.07	646.40	-2.22
$DRE = F_{cloud}^{\uparrow} - F_{cloud+aer}^{\uparrow}$	92.06	81.92	-11.01

4 **Table 2.** Fluxes for polluted and clean scene and DRE ($\text{W}\cdot\text{m}^{-2}\cdot\mu\text{m}^{-1}$) at the TOA at $0.490 \mu\text{m}$ modeled using a 3D and 1D
5 assumption.

F. Peers 23/2/y 17:33

Supprimé: .

F. Peers 23/2/y 17:33

Supprimé: 1 –

F. Peers 23/2/y 17:33

Supprimé: microphysical

F. Peers 23/2/y 17:33

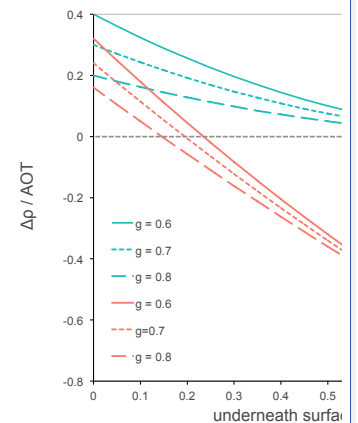
Supprimé: for RT simulations (left) and retrieved by

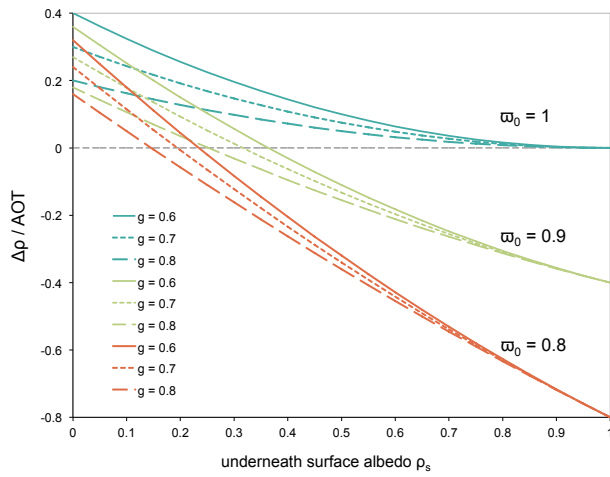
F. Peers 23/2/y 17:33

Supprimé: (right) for several refractive indexes ($n = m - i.k$) of fine mode aerosols. Aerosol properties are given at 865 nm and the Cloud Optical Thickness at 550 nm

F. Peers 23/2/y 17:33

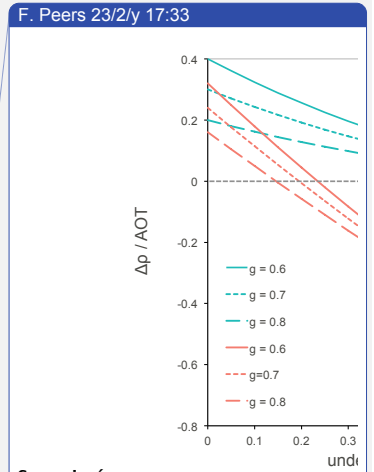
Supprimé: Table 2 – Same as Table 1 for several angström exponents α of DUST aerosols.



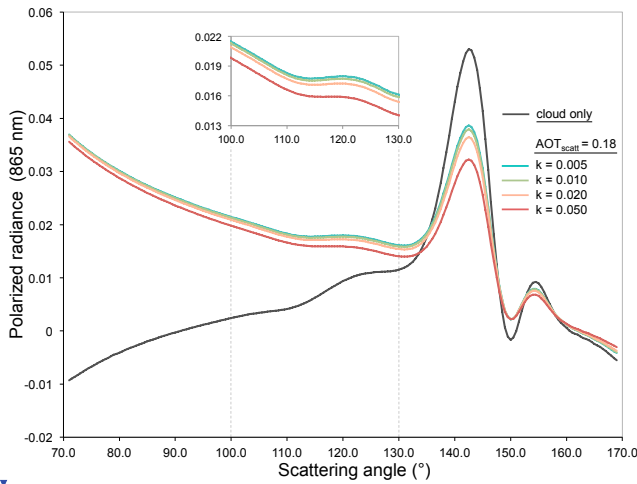


1
2
3
4
5

Figure 1. Modification of the albedo of a scene $\Delta\rho$ caused by the presence of an aerosol layer versus the albedo of the underneath surface ρ_s calculated with the approximate expression given by Lenoble et al. [1982]. [Dark green](#) lines correspond to [purely scattering only aerosols](#) ($\omega_0 = 1$), [light green](#) to [aerosols moderately absorbing](#) ($\omega_0 = 0.9$) and orange lines are for [absorbing aerosols](#) ($\omega_0 = 0.8$) and g is the asymmetry factor.

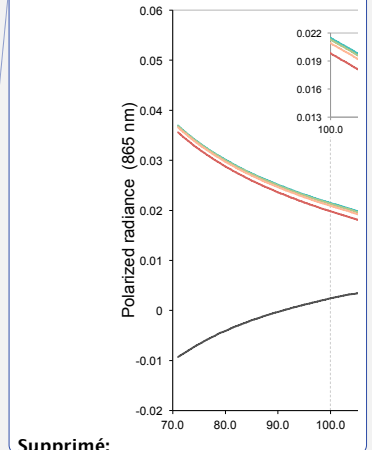


Supprimé:
F. Peers 23/2/y 17:33
Supprimé: -
F. Peers 23/2/y 17:33
Supprimé: Green
F. Peers 23/2/y 17:33

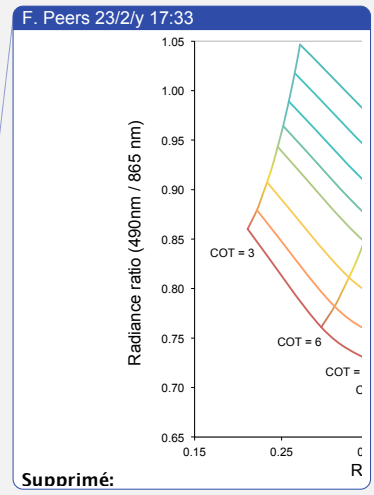
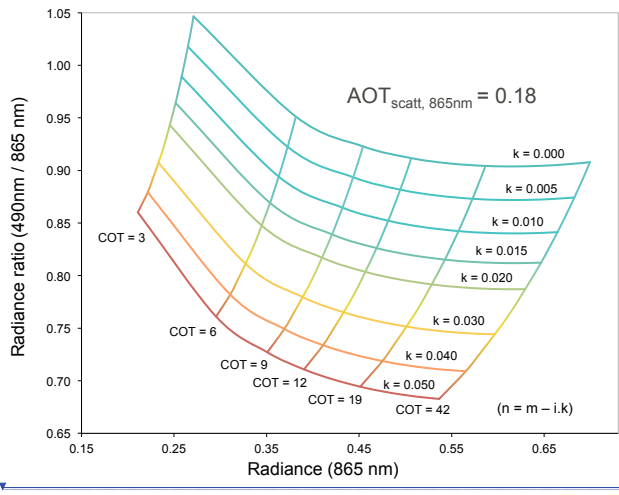


6
7
8
9
10
11

Figure 2. Simulated polarized radiance at 865 nm plotted against the scattering angle. Black line corresponds to the cloud only ($COT_{\nu} = 10$, $r_{eff} = 10 \mu m$). Colored lines are for an aerosol layer above clouds. The effective radius of aerosols is $0.10 \mu m$. Several absorption AOT (i.e. various k) have been considered but the scattering AOT is fixed at 0.18. [The inset focuses on polarized radiances of aerosols above clouds for scattering angles between 100° and 130°](#). Complementary information about vertical distributions and properties of aerosols and clouds can be found in Table 1 (cf. polarized LUT).

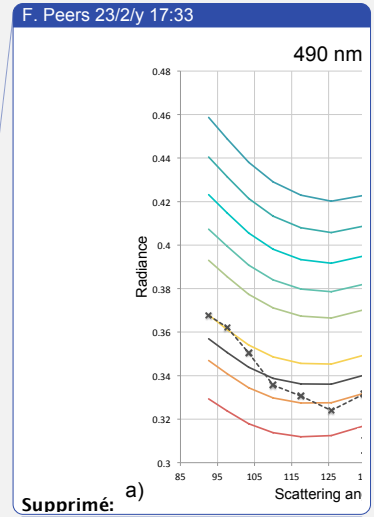


Supprimé:
F. Peers 23/2/y 17:33
Supprimé: -
F. Peers 23/2/y 17:33
Supprimé: =
F. Peers 23/2/y 17:33
Supprimé: =
F. Peers 23/2/y 17:33
Supprimé:
F. Peers 23/2/y 17:33
Supprimé:



F. Peers 23/2/y 17:33
Supprimé: -

F. Peers 23/2/y 17:33
Supprimé: for a solar zenith angle of 40°.



Supprimé:
F. Peers 23/2/y 17:33
Supprimé: -

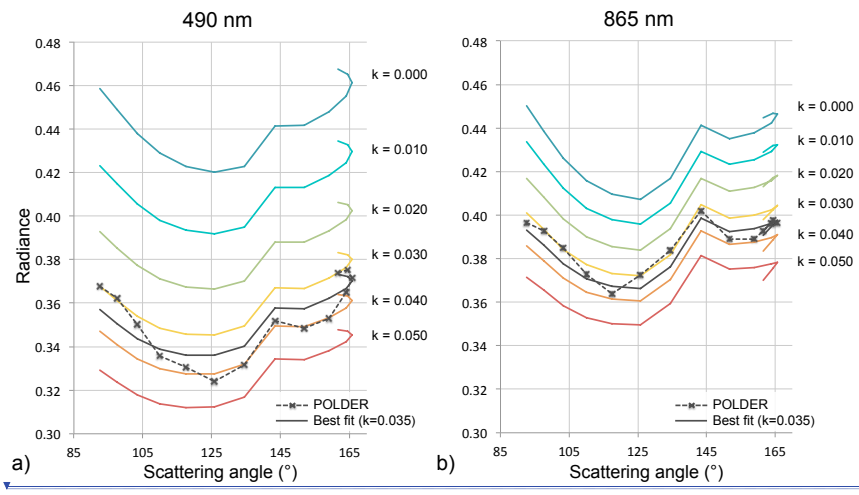
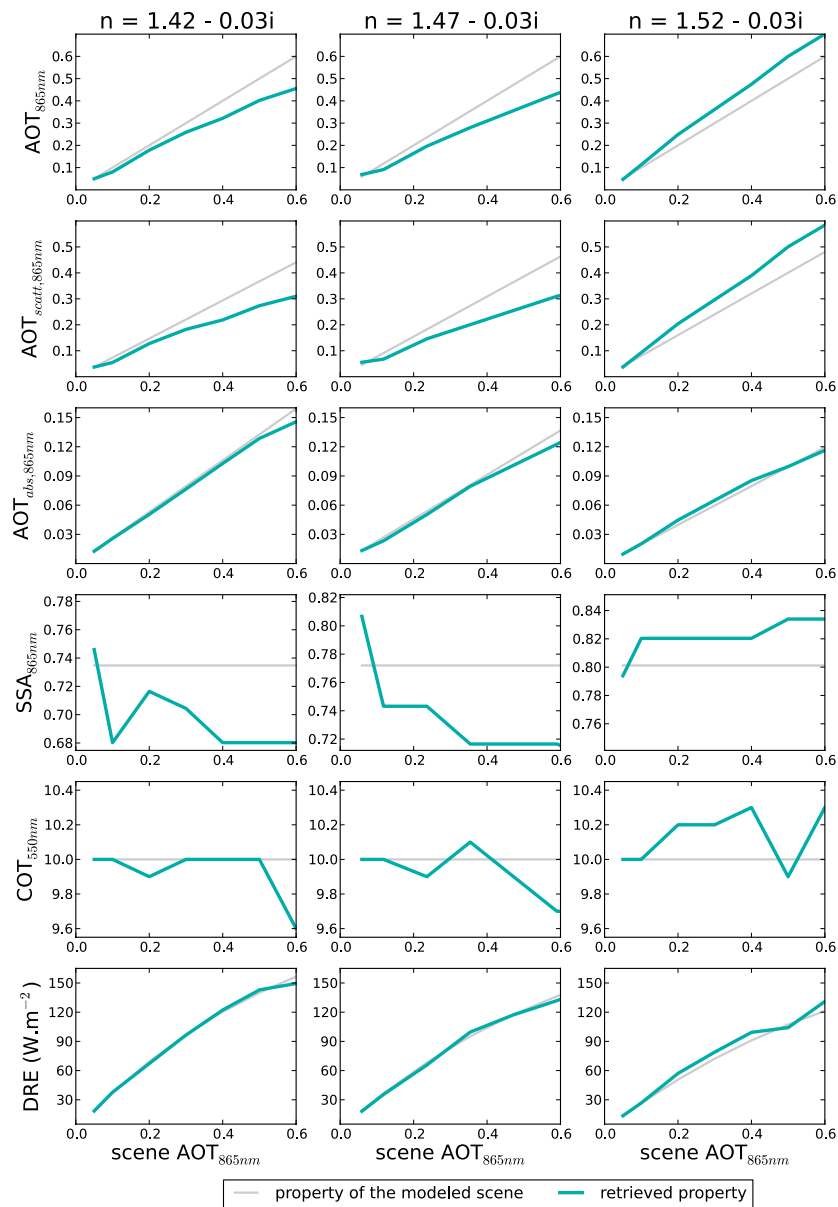


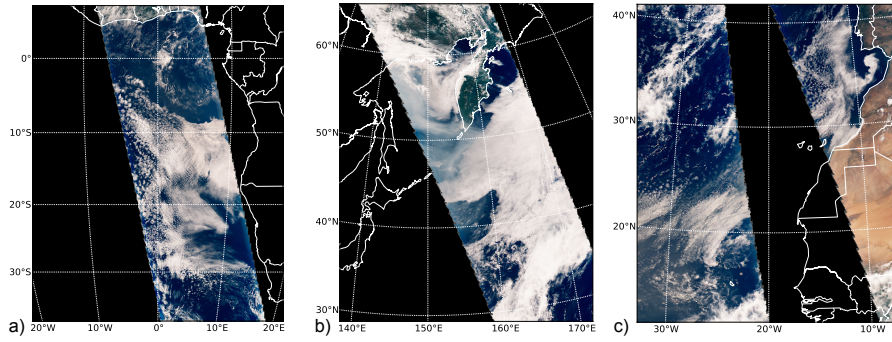
Figure 3. Radiance ratio L_{490nm}/L_{865nm} as a function of the radiance at 865 nm. Signals have been simulated for aerosols with an effective radius of $0.10 \mu m$, an effective radius of cloud droplet of $10 \mu m$ (for more information about aerosol and cloud properties and vertical distribution, cf. Table 1, total radiance LUT column). The scattering AOT is set and several absorption AOT as well as several COT are considered. Calculations have been carried out for a solar zenith angle $\theta_s = 41.3^\circ$, a viewing angle $\theta_v = 41.3^\circ$ and a relative azimuth $\phi_r = 180^\circ$.

Figure 4. Example of measured and simulated total radiances for one pixel at 490 nm (a) and 865 nm (b). The dashed black lines are for the measurements and the continuous black ones are for the simulated signals corresponding to the solution (i.e. COT = 12.4; $k = 0.035$; AOT = 0.14). Other colored lines correspond to the signal simulated for the same COT, the same scattering AOT and for several k (i.e. different absorption AOT).

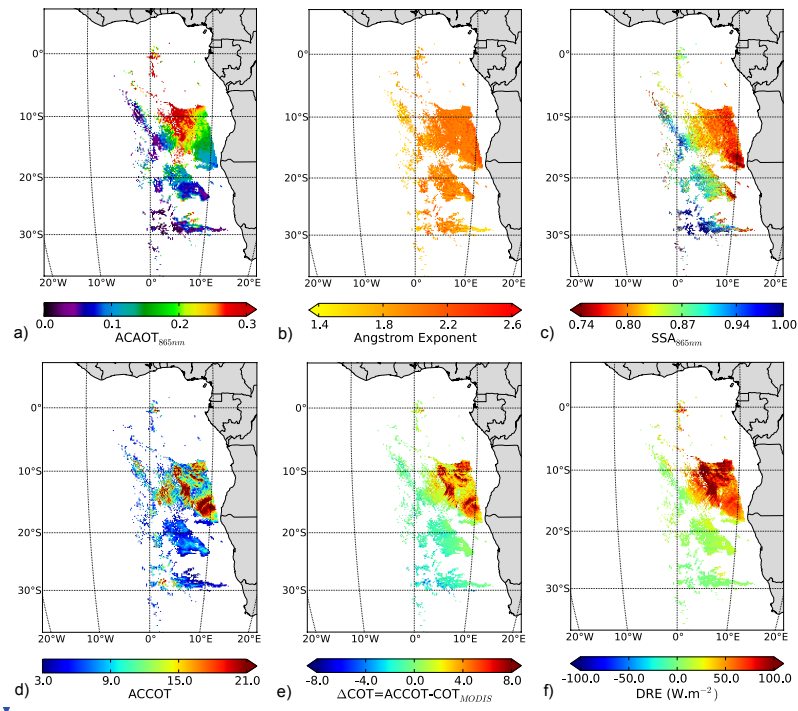


1

2 **Figure 5.** Sensitivity of the properties of an AAC scene with different aerosol models. From top to the bottom: total AOT,
 3 scattering AOT, absorption AOT and SSA at 865 nm, COT at 550 nm and the short wave DRE of aerosols. Grey lines
 4 correspond to the properties of the actual modeled scene and green lines to those retrieved by the algorithm. The aerosol
 5 model of the first column has a refractive index n equal to $1.42 - 0.03i$, the second, $n = 1.47 - 0.03i$ and the third,
 6 $n = 1.52 - 0.03i$. Aerosols have an effective radius of $0.1 \mu\text{m}$ and the effective radius of the cloud water droplets is $10 \mu\text{m}$.



1
2 **Figure 6.** True color POLDER/PARASOL RGB composite (a) over the South East Atlantic Ocean the 4th of August 2008,
3 (b) off the East Russian coast the 3rd of July 2008 and (c) over the North Atlantic Ocean the 4th of August 2008.



4
5 **Figure 7.** Biomass burning aerosols above clouds off the South West African Coast on 4th August 2008. The panel displays
6 the Above Cloud AOT at 865 nm (a), the Angström Exponent (b), the aerosol SSA at 865 nm (c), the Aerosol Corrected COT
7 at 550 nm (d), the difference ΔCOT of the AACOT and the MODIS COT (e) and the Direct Radiative Effect of aerosols
8 above clouds in $W \cdot m^{-2}$ (f).

F. Peers 23/2/y 17:33

Supprimé: ... [2]

F. Peers 23/2/y 17:33

Supprimé: 6 – Aerosol and cloud properties and DRE for biomass

F. Peers 23/2/y 17:33

Supprimé: ACA events

F. Peers 23/2/y 17:33

Supprimé: coast the

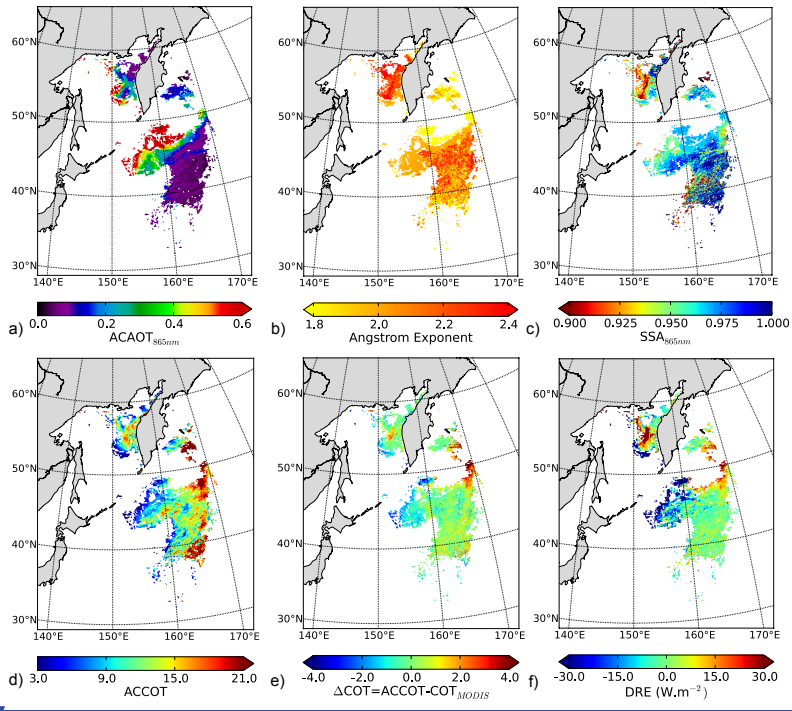
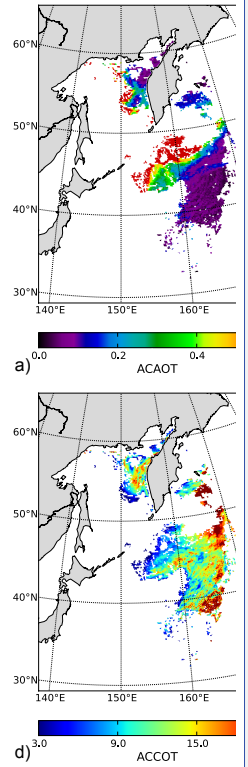


Figure 8. Same as Fig. 7 for biomass burning aerosols from Siberia on 3rd July 2008.

F. Peers 23/2/y 17:33



Supprimé:

F. Peers 23/2/y 17:33

Supprimé: 7 -

F. Peers 23/2/y 17:33

Supprimé: Figure 6

F. Peers 23/2/y 17:33

Supprimé: the

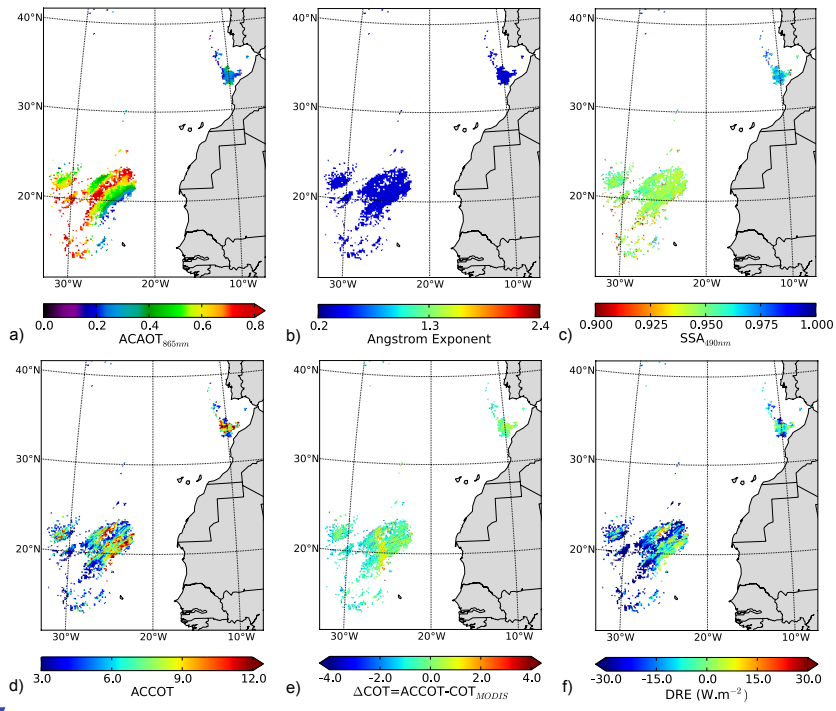
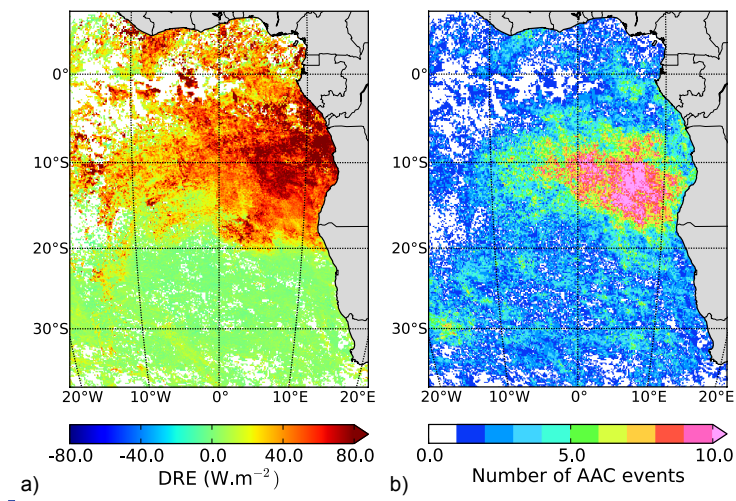


Figure 9. Same as Fig. 7 for Saharan dust above clouds on 4th August 2008, except Fig. 9c that displays the aerosol SSA at 490 nm.



F. Peers 23/2/y 17:33

Supprimé: -

... [3]

F. Peers 23/2/y 17:33

Supprimé: 8 -

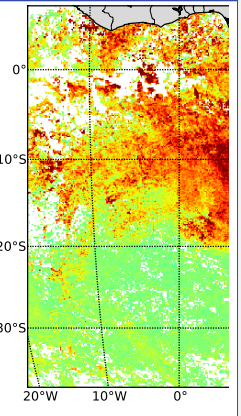
F. Peers 23/2/y 17:33

Supprimé: Figure 6

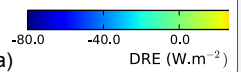
F. Peers 23/2/y 17:33

Supprimé: the

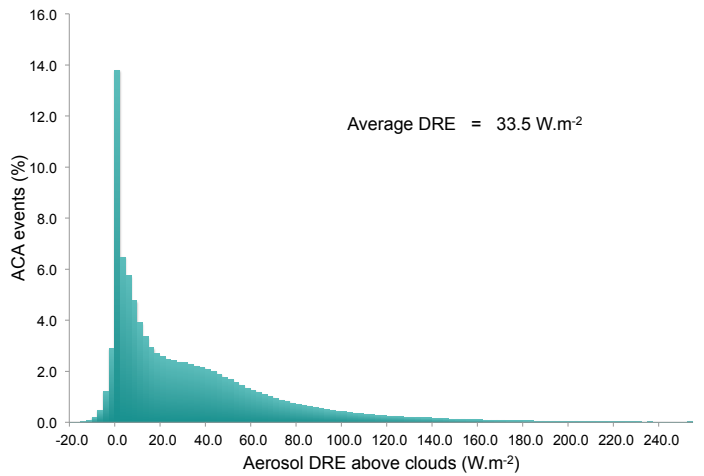
F. Peers 23/2/y 17:33



Supprimé: a)



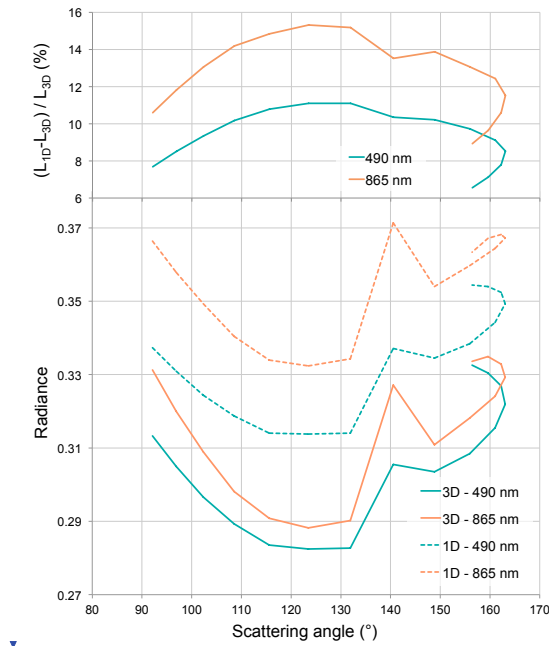
1 **Figure 10.** Direct Radiative Effect of aerosols above clouds averaged through August 2006 (a) and number of associated
 2 events (b). The DRE has been processed over scenes with a Cloud Fraction (CF) equal to 1 and COT ≥ 3 .



F. Peers 23/2/y 17:33

Supprimé: 9 -

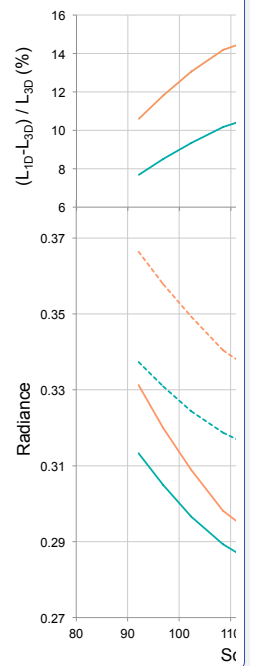
3
 4 **Figure 11.** Frequency distribution of the aerosol Direct Radiative Effect above clouds for August 2006 for the South East
 5 Atlantic Ocean. Only scenes with COT ≥ 3 and CF = 1 are considered.



F. Peers 23/2/y 17:33

Supprimé: 10 -

F. Peers 23/2/y 17:33



Supprimé:

6

- 1 | **Figure 12.** Simulated radiances for aerosols above a heterogeneous cloud ($\sigma(\text{COT})/\text{COT} = 0.6$) at 490 nm (green lines) and
- 2 | 865 nm (orange lines) for a solar zenith angle of 40° . 3D signals (continuous lines) have been obtained thanks to the
- 3 | 3DMCPOL code and based on a cloud field modeled with 3DCLOUD.

F. Peers 23/2/y 17:33

Supprimé: 11 –